AN ENERGY STABLE FINITE DIFFERENCE SCHEME FOR THE ERICKSEN-LESLIE SYSTEM WITH PENALTY FUNCTION AND ITS OPTIMAL RATE CONVERGENCE ANALYSIS*

KELONG CHENG†, CHENG WANG‡, AND STEVEN M. WISE§

Abstract. A first-order-accurate-in-time, finite difference scheme is proposed and analyzed for the Ericksen-Leslie system, which describes the evolution of nematic liquid crystals. For the penalty function to approximate the constraint $|\boldsymbol{d}| = 1$, a convex-concave decomposition for the corresponding energy functional is applied. In addition, appropriate semi-implicit treatments are adopted for the convection terms, for both the velocity vector and orientation vector, as well as the coupled elastic stress terms. In turn, all the semi-implicit terms can be represented as a linear operator of a vector potential, and its combination with the convex splitting discretization for the penalty function leads to a unique solvability analysis for the proposed numerical scheme. Furthermore, a careful estimate reveals an unconditional energy stability of the numerical system, composed of the kinematic energy and internal elastic energies. More importantly, we provide an optimal rate convergence analysis and error estimate for the numerical scheme. In addition, a nonlinear iteration solver is outlined, and the numerical accuracy test results are presented, which confirm the optimal rate convergence estimate.

Keywords. Ericksen-Leslie system with the penalty function; convex-concave decomposition; unique solvability; energy stability; staggered mesh points; optimal rate convergence analysis.

AMS subject classifications. 35K55; 65M06; 65M12; 76D05.

1. Introduction

In this article, we examine the following macroscopic hydrodynamical model of nematic liquid crystals for materials with isotropic elastic energies, derived by Ericksen and Leslie [16, 21]:

$$\partial_t \boldsymbol{u} + \boldsymbol{u} \cdot \nabla \boldsymbol{u} + \nabla p - \nu \Delta \boldsymbol{u} - \lambda \nabla \cdot \Big(-(\nabla \boldsymbol{d})^T \nabla \boldsymbol{d}$$
$$+ \beta (\Delta \boldsymbol{d} - \boldsymbol{f}(\boldsymbol{d})) \boldsymbol{d}^T + (\beta + 1) \boldsymbol{d} (\Delta \boldsymbol{d} - \boldsymbol{f}(\boldsymbol{d}))^T \Big) = 0, \tag{1.1}$$

$$\nabla \cdot \boldsymbol{u} = 0, \tag{1.2}$$

$$\partial_t \boldsymbol{d} + \boldsymbol{u} \cdot \nabla \boldsymbol{d} + (\beta \nabla \boldsymbol{u} + (1 + \beta)(\nabla \boldsymbol{u})^T) \boldsymbol{d} = \gamma (\Delta \boldsymbol{d} - \boldsymbol{f}(\boldsymbol{d})), \tag{1.3}$$

with initial and boundary conditions

$$\boldsymbol{u}\,|_{t=0} = \boldsymbol{u}_0, \quad \boldsymbol{d}\,|_{t=0} = \boldsymbol{d}_0, \quad \boldsymbol{u} \cdot \boldsymbol{n}|_{\partial \Omega} = \boldsymbol{d} \cdot \boldsymbol{n}|_{\partial \Omega} = 0, \quad \frac{\partial(\boldsymbol{u} \cdot \tau)}{\partial \boldsymbol{n}}\bigg|_{\partial \Omega} = \frac{\partial(\boldsymbol{d} \cdot \tau)}{\partial \boldsymbol{n}}\bigg|_{\partial \Omega} = 0. \tag{1.4}$$

The vector $\boldsymbol{u} = (u, v, w)^T$ represents the velocity of the liquid crystal flow; p is the pressure; $\boldsymbol{d} = (d_1, d_2, d_3)^T$ is the orientation of the liquid crystal molecules; $\beta \in [-1, 0]$ is a constant; the parameter $\nu > 0$ is the fluid viscosity coefficient constant; $\lambda > 0$ is an

elastic constant; and $\gamma > 0$ is a relaxation time constant. The vector function $\boldsymbol{f}(\boldsymbol{d})$ may be viewed as a penalty function to approximate the constraint $|\boldsymbol{d}| = 1$:

$$\boldsymbol{f}(\boldsymbol{d}) = \varepsilon^{-2}(|\boldsymbol{d}|^2 - 1)\boldsymbol{d}. \tag{1.5}$$

This penalty term is physically meaningful and stands for a possible relaxation of molecules from the strict unit-length constraint. Such an approach could also be viewed as a regularization method when compared with the limit system, where $|\boldsymbol{d}| = 1$ is rigidly imposed.

Here, the chemical potential $\boldsymbol{\mu} = \boldsymbol{f}(\boldsymbol{d}) - \Delta\boldsymbol{d} = (\mu_1, \mu_2, \mu_3)^T$ is a column vector, with the following components:

$$\mu_i = \varepsilon^{-2}(|\boldsymbol{d}|^2 - 1)d_i - \Delta d_i, \quad i = 1, 2, 3. \tag{1.6}$$

Let us recall the following identity,

$$\nabla \cdot \left((\nabla \boldsymbol{d})^T \nabla \boldsymbol{d} \right) = \sum_{i=1}^{3} \sum_{j=1}^{3} \frac{\partial}{\partial x_j} \left(\sum_{k=1}^{3} \frac{\partial d_k}{\partial x_i} \frac{\partial d_k}{\partial x_j} \right) \hat{\boldsymbol{e}}_i \tag{1.7}$$

$$= \Delta d_1 \nabla d_1 + \Delta d_2 \nabla d_2 + \Delta d_3 \nabla d_3 + \frac{1}{2}\nabla(|\nabla\boldsymbol{d}|^2)$$

$$= d_1 \nabla\mu_1 + d_2 \nabla\mu_2 + d_3 \nabla\mu_3 + \nabla\pi \tag{1.8}$$

$$= (\nabla\boldsymbol{\mu})^T \boldsymbol{d} + \nabla\pi, \tag{1.9}$$

where

$$\pi := \frac{1}{2}|\nabla\boldsymbol{d}|^2 + \boldsymbol{d} \cdot \Delta\boldsymbol{d} - \frac{1}{4}(|\boldsymbol{d}|^2 - 1)^2 - \frac{1}{2}|\boldsymbol{d}|^2.$$

Then we are able to rewrite the original PDE system as

$$\partial_t \boldsymbol{u} + \boldsymbol{u} \cdot \nabla\boldsymbol{u} + \nabla p' - \nu\Delta\boldsymbol{u} + \lambda(\nabla\boldsymbol{\mu})^T \boldsymbol{d} + \lambda\nabla \cdot \left(\beta\boldsymbol{\mu}\boldsymbol{d}^T + (\beta+1)\boldsymbol{d}\boldsymbol{\mu}^T \right) = 0, \tag{1.10}$$

$$\nabla \cdot \boldsymbol{u} = 0, \tag{1.11}$$

$$\partial_t \boldsymbol{d} + \boldsymbol{u} \cdot \nabla\boldsymbol{d} + (\beta\nabla\boldsymbol{u} + (1+\beta)(\nabla\boldsymbol{u})^T)\boldsymbol{d} = -\gamma\boldsymbol{\mu}, \tag{1.12}$$

where $p' = p + \lambda\pi$ is a modified pressure. For simplicity, we will use the modified pressure but drop the prime notation.

Now, let us introduce a free energy for the orientation vector field $\boldsymbol{d}$:

$$E(\boldsymbol{d}) = \int_\Omega \varepsilon^{-2}\left(\frac{1}{4}|\boldsymbol{d}|^4 - \frac{1}{2}|\boldsymbol{d}|^2 \right) + \frac{1}{2}|\nabla\boldsymbol{d}|^2 \, d\mathbf{x}. \tag{1.13}$$

We observe that $d_t E(\boldsymbol{d}) = \int_\Omega \partial_t \boldsymbol{d} \cdot \boldsymbol{\mu} \, d\mathbf{x}$. Taking inner products of (1.10) with $\boldsymbol{u}$ and (1.12) with $\lambda\boldsymbol{\mu}$, we get the remarkable energy dissipation law:

$$\partial_t E(\boldsymbol{d}, \boldsymbol{u}) = -\nu\|\nabla\boldsymbol{u}\|^2 - \gamma\|\boldsymbol{\mu}\|^2 \leq 0, \quad E(\boldsymbol{d}, \boldsymbol{u}) := \frac{1}{2}\|\boldsymbol{u}\|^2 + \lambda E(\boldsymbol{d}). \tag{1.14}$$

A theoretical analysis for the coupled PDE system and its limit system has been established in [32–34, 51, 52]; also see the related works [38–40, 47], *et cetera*.

There have been extensive numerical works for the Ericksen-Leslie system, both for the penalty formulation and the constraint formulation, in the existing literature [1, 7,

8, 15, 18, 28, 29, 49, 53–55]. In particular, the energy stability property of the numerical schemes has attracted a great deal of attention in recent years. Various semi-discrete finite element schemes were analyzed in [35–37], with energy dissipation law established. Among the fully discrete approaches, an energy stable time splitting method is proposed and analyzed in [5], in which the coupled elastic stress terms were not considered in the system. Further development of energy stability has been reported in more recent works [56–58], in which both the first and second order accurate energy stable schemes were studied for the full coupled system (1.1)-(1.3).

Meanwhile, it is observed that, an optimal rate convergence analysis for the full Ericksen-Leslie system (1.1)-(1.3) has been a very challenging theoretical issue. Among the existing theoretical works, it is worthy of mentioning [2], in which a fully discrete finite element scheme to a simplified system (without the coupled elastic stress terms, $\beta(\nabla \boldsymbol{u})\boldsymbol{d}$ and $(1+\beta)(\nabla \boldsymbol{u})^T\boldsymbol{d}$) is analyzed. The numerical convergence is proved by establishing a uniform bound for the numerical solution (in terms of time step and numerical mesh grid sizes) and taking a weak limit via certain compactness arguments, while an optimal rate error estimate has not been reported. Moreover, the convergence towards measure-valued solutions of the limiting Ericksen-Leslie model has been established in [2], which turns out to be another significant theoretical result. As a further development, a fully discrete, mixed finite element numerical scheme was proposed for the penalized Ericksen-Leslie system in [26], in which the nonlinear terms are treatment in a semi-implicit manner. In particular, an optimal rate convergence analysis was reported in [26], with first order convergence rate in both time and space. It is noticed that the standard L^2 and H^1 bounds for the numerical solution have been derived, while an energy dissipation (in terms of the physical energy) was not reported. In a subsequent work [27], a modified energy stability was proved for the mixed finite element schemes, with an "initial estimate" constraint $h \leq C\varepsilon$ and the "stability" constraint $\Delta t = O(\varepsilon^2 h^2)$. Also see the related works [1, 35, 37]. Furthermore, in some recent works for related phase field models of nematic liquid crystal droplets [3, 18, 43, 44, 48], the energy dissipation analysis has been reported for the finite element schemes, and the Γ-convergence of global discrete energy minimizers of the numerical solution to global minimizers of the continuous energy has been proved. Many deep and subtle techniques have been included in these theoretical analyses.

In this paper we propose a finite difference scheme for the full Ericksen-Leslie system (1.1)-(1.3), with the coupled elastic stress terms included, and we provide an optimal rate convergence analysis, with first order accuracy in time and second order accuracy in space. For the vector penalty function (1.5), a convex splitting algorithm is applied to the corresponding elastic energy functional. Meanwhile, for all the coupled terms, $(\nabla \boldsymbol{\mu})^T\boldsymbol{d}$, $\nabla \cdot (\boldsymbol{\mu} \boldsymbol{d}^T)$, $\nabla \cdot (\boldsymbol{d} \boldsymbol{\mu}^T)$, $\boldsymbol{u} \cdot \nabla \boldsymbol{d}$, $(\nabla \boldsymbol{u})\boldsymbol{d}$, $(\nabla \boldsymbol{u})^T\boldsymbol{d}$, we have to make use of appropriate semi-implicit discretization. All of these semi-implicit terms could be represented as a linear operator of the vector potential $\boldsymbol{\mu}$ at time step at t^{n+1}. A combination of such a linear operator representation and the convex splitting discretization for $\boldsymbol{d}$ in the vector chemical potential $\boldsymbol{\mu}$ results in a unique solvability analysis for the proposed numerical scheme, with the help of Browder-Minty lemma, based on the monotonicity property of the numerical system. In addition, an unconditional energy stability of the numerical scheme could be derived, in which both the convex splitting treatment for $\boldsymbol{d}$ and semi-implicit approximation for the coupled terms will play an important role in the energy stability estimate.

In terms of the optimal convergence analysis, the primary challenge is associated with the error estimates for these coupled terms, including the convection and elastic

stress terms. Although the semi-implicit treatment makes a linear operator in terms of $\boldsymbol{\mu}$, the corresponding error estimate turns out to be highly nonlinear. Furthermore, a careful calculation implies that, the standard diffusion term for either the velocity or the phase field is not able to control the numerical error associated with the nonlinear coupled terms.

To overcome this subtle difficulty, we perform an $L^\infty_{\Delta t}(0,T;H^1) \cap L^2_{\Delta t}(0,T;H^2)$ error estimate for the phase variable $\boldsymbol{d}$, combined with an $L^\infty_{\Delta t}(0,T;L^2) \cap L^2_{\Delta t}(0,T;H^1)$ error estimate for the velocity vector. Such an estimate in a higher order Sobolev norm is necessary to make three nonlinear coupled inner products (with appropriate error test function) be cancelled between the momentum and phase field error equations. This observation could not be obtained through a standard $L^\infty_{\Delta t}(0,T;L^2) \cap L^2_{\Delta t}(0,T;H^1)$ error estimate for the phase variable. Similar techniques have been reported in the convergence analysis for various Cahn-Hilliard-Fluid (such as Cahn-Hilliard-Hele-Shaw or Cahn-Hilliard-Navier-Stokes) models [6, 9, 10, 17, 19, 41]; meanwhile, the technical details presented in this work are much more complicated than the ones in these recent works for the Cahn-Hilliard-Fluid models, since only one coupled term appears in the phase field equation of the latter one, in comparison with three terms in the Eriksen-Leslie system.

In addition, for the fully discrete scheme, the discrete Sobolev embeddings from H^1_h into L^4_h and L^6_h (in the finite difference space) will also play an important role in the nonlinear error estimate. Such a discrete inequality could not be obtained via a direct local calculation; instead, a discrete Fourier expansion for the test function (with given boundary condition), combined with careful eigenvalue estimates, is needed for the derivation. Also see the related recent works [12, 14, 22–24].

This paper is organized as follows. In Section 2 we propose the fully-discrete numerical method, outline the staggered finite difference spatial approximation, as well as the temporal discretization, and prove the unique solvability of the scheme. The energy stability analysis is provided in Section 3. An optimal rate convergence analysis is established in Section 4. A nonlinear iteration solver is outlined, and numerical accuracy test results are presented in Section 5. Finally, some concluding remarks are made in Section 6.

2. The numerical scheme

2.1. Finite difference spatial discretization.   For simplicity of presentation, we focus our discussions on the two-dimensional (2-D) case, with the computational domain given by $\Omega = (0,1)^2$. An extension to the three-dimensional (3-D) case is straightforward, and the details are left to the interested readers.

It is assumed that N is a positive integer such that $h = \frac{1}{N}$, which is called the spatial step size. The orientation vector field $\boldsymbol{d}$ is evaluated at the cell-centered mesh points: $((i+1/2)h,(j+1/2)h)$, at the component-wise level. In turn, the discrete gradient of $\boldsymbol{d}$ is evaluated at the mesh points $(ih,(j+1/2)h)$, $((i+1/2)h,jh)$, respectively:

$$
\begin{aligned}
(D_x d_k)_{i,j+1/2} &= \frac{(d_k)_{i+1/2,j+1/2} - (d_k)_{i-1/2,j+1/2}}{h}, \\
(D_y d_k)_{i+1/2,j} &= \frac{(d_k)_{i+1/2,j+1/2} - (d_k)_{i+1/2,j-1/2}}{h},
\end{aligned}
\tag{2.1}
$$

for $k=1,2$. The five-point Laplacian takes a standard form. The pressure field p and chemical potential vector field $\boldsymbol{\mu}$ are also evaluated at the cell-centered mesh points, and the discrete gradient could be defined in the same way as in (2.1). Similarly, the

wide-stencil differences for cell-centered functions could be introduced as

$$(\tilde{D}_x \mu_k)_{i+1/2,j+1/2} = \frac{(\mu_k)_{i+3/2,j+1/2} - (\mu_k)_{i-1/2,j+1/2}}{2h},$$

$$(\tilde{D}_y \mu_k)_{i+1/2,j+1/2} = \frac{(\mu_k)_{i+1/2,j+3/2} - (\mu_k)_{i+1/2,j-1/2}}{2h}. \tag{2.2}$$

Meanwhile, in order to assure the divergence-free property of the velocity vector at the discrete level, we choose a staggered grid for the velocity field, in which the individual components of a given velocity, say, $\boldsymbol{v} = (v^x, v^y)$, are defined at the east-west cell edge points $(ih, (j+1/2)h)$, and the north-south cell edge points $((i+1/2)h, jh)$, respectively. This staggered grid is also known as the marker and cell (MAC) grid and was first proposed in [31] to deal with the incompressible Navier-Stokes equations, and the detailed analyses have been provided in [20, 50]. Also see the related applications to the primitive equations [45] and planetary geostrophic equations [46], *et cetera*.

The discrete divergence of $\boldsymbol{v}$, specifically,

$$\nabla_h \cdot \boldsymbol{v} = D_x v^x + D_y v^y,$$

is defined at the cell center points $((i+1/2)h, (j+1/2)h)$ as follows:

$$(\nabla_h \cdot \boldsymbol{v})_{i+1/2,j+1/2} := (D_x v^x)_{i+1/2,j+1/2} + (D_y v^y)_{i+1/2,j+1/2}.$$

One key advantage of the MAC grid approach is that the discrete divergence of the unknown grid velocity will always be identically zero at every cell center point. Such a divergence-free property at the discrete level comes from the special structure of the MAC grid and assures that the velocity field is orthogonal to a corresponding discrete pressure gradient at the discrete level; see also reference [20].

Moreover, we observe that the velocity component v^x has zero boundary values at mesh points $(0, (j+1/2)h)$ and $(Nh, (j+1/2)h)$, corresponding to the boundaries at $x=0$ and $x=1$. Similarly, the velocity component v^y has zero boundary values at mesh points $((i+1/2)h, 0)$ and $((i+1/2)h, Nh)$, so that the boundary condition of $\boldsymbol{n} \cdot \boldsymbol{v} = 0$ is satisfied at the point-wise (global) level at all four boundary faces.

A discrete cell-centered function ϕ is said to satisfy homogeneous Neumann boundary conditions, and we write $\boldsymbol{n} \cdot \nabla_h \phi = 0$ iff at the ghost points ϕ satisfies

$$\phi_{-1/2,j+1/2} = \phi_{1/2,j}, \quad \phi_{N+1/2,j+1/2} = \phi_{N-1/2,j+1/2},$$

$$\phi_{i+1/2,-1/2} = \phi_{i+1/2,1/2}, \quad \phi_{i+1/2,N+1/2} = \phi_{i+1/2,N-1/2}. \tag{2.3}$$

A discrete function $\boldsymbol{f} = (f^x, f^y)^T \in \vec{\mathcal{E}}_\Omega$ is said to satisfy the homogeneous boundary conditions $\boldsymbol{n} \cdot \boldsymbol{f} = 0$ iff we have

$$f^x_{-1/2,j+1/2} + f^x_{1/2,j+1/2} = 0, \ f^x_{N+1/2,j+1/2} + f^x_{N-1/2,j+1/2} = 0, \tag{2.4}$$

$$f^y_{i+1/2,1/2} + f^y_{i+1/2,-1/2} = 0, \ f^y_{i+1/2,N+1/2} + f^y_{i+1/2,N-1/2} = 0. \tag{2.5}$$

For $\boldsymbol{u} = (u^x, u^y)^T$, $\boldsymbol{v} = (v^x, v^y)^T$, located at the staggered mesh points $(x_i, y_{j+1/2})$, $(x_{i+1/2}, y_j)$, respectively, and the cell-centered vector field $\boldsymbol{d} = (d^x, d^y)^T$, $\boldsymbol{\mu} = (\mu^x, \mu^y)^T$, the following terms are evaluated as

$$\boldsymbol{u} \cdot \nabla_h \boldsymbol{v} = \begin{pmatrix} u^x_{i,j+1/2} \tilde{D}_x v^x_{i,j+1/2} + \mathcal{A}_{xy} u^y_{i,j+1/2} \tilde{D}_y v^x_{i,j+1/2} \\ \mathcal{A}_{xy} u^x_{i+1/2,j} \tilde{D}_x v^y_{i+1/2,j} + u^y_{i,j+1/2} \tilde{D}_y v^y_{i+1/2,j} \end{pmatrix}, \tag{2.6}$$

$$\nabla_h \cdot (\boldsymbol{vu}^T) = \begin{pmatrix} \tilde{D}_x(u^x v^x)_{i,j+1/2} + \tilde{D}_y(\mathcal{A}_{xy} u^y v^x)_{i,j+1/2} \\ \tilde{D}_x(\mathcal{A}_{xy} u^x v^y)_{i+1/2,j} + \tilde{D}_y(u^y v^y)_{i+1/2,j} \end{pmatrix}, \tag{2.7}$$

$$(\nabla_h \boldsymbol{\mu})^T \boldsymbol{d} = \begin{pmatrix} (D_x \mu^x \cdot \mathcal{A}_x d^x)_{i,j+1/2} + (D_x \mu^x \cdot \mathcal{A}_x d^y)_{i,j+1/2} \\ (D_y \mu^x \cdot \mathcal{A}_y d^x)_{i+1/2,j} + (D_y \mu^y \cdot \mathcal{A}_y d^y)_{i+1/2,j} \end{pmatrix}, \tag{2.8}$$

$$\nabla_h \cdot (\boldsymbol{\mu d}^T) = \begin{pmatrix} D_x(\mu^x d^x)_{i,j+1/2} + \mathcal{A}_x \tilde{D}_y(\mu^x d^y)_{i,j+1/2} \\ \mathcal{A}_y \tilde{D}_x(\mu^y d^x)_{i+1/2,j} + D_y(\mu^y d^y)_{i+1/2,j} \end{pmatrix}, \tag{2.9}$$

$$\nabla_h \cdot (\boldsymbol{d\mu}^T) = \begin{pmatrix} D_x(\mu^x d^x)_{i,j+1/2} + \mathcal{A}_x \tilde{D}_y(\mu^y d^x)_{i,j+1/2} \\ \mathcal{A}_y \tilde{D}_x(\mu^x d^y)_{i+1/2,j} + D_y(\mu^y d^y)_{i+1/2,j} \end{pmatrix}, \tag{2.10}$$

$$\nabla_h \cdot (\boldsymbol{du}^T) = \begin{pmatrix} D_x(\mathcal{A}_x d^x u^x)_{i+1/2,j+1/2} + D_y(\mathcal{A}_y d^x u^y)_{i+1/2,j+1/2} \\ D_x(\mathcal{A}_x d^y u^x)_{i+1/2,j+1/2} + D_y(\mathcal{A}_y d^y u^y)_{i+1/2,j+1/2} \end{pmatrix}, \tag{2.11}$$

$$(\nabla_h \boldsymbol{u}) \boldsymbol{d} = \begin{pmatrix} (D_x u^x \cdot d^x)_{i+1/2,j+1/2} + (\mathcal{A}_x \tilde{D}_y u^x \cdot d^y)_{i+1/2,j+1/2} \\ (\mathcal{A}_y \tilde{D}_x u^y \cdot d^x)_{i+1/2,j+1/2} + (D_y u^y \cdot d^y)_{i+1/2,j+1/2} \end{pmatrix}, \tag{2.12}$$

$$(\nabla_h \boldsymbol{u})^T \boldsymbol{d} = \begin{pmatrix} (D_x u^x \cdot d^x)_{i+1/2,j+1/2} + (\mathcal{A}_y \tilde{D}_x u^y \cdot d^y)_{i+1/2,j+1/2} \\ (\mathcal{A}_x \tilde{D}_y u^x \cdot d^x)_{i+1/2,j+1/2} + (D_y u^y \cdot d^y)_{i+1/2,j+1/2} \end{pmatrix}, \tag{2.13}$$

where the following averaging operators have been employed:

$$\mathcal{A}_{xy} u^x_{i+1/2,j} = \frac{1}{4} \left(u^x_{i,j-1/2} + u^x_{i,j+1/2} + u^x_{i+1,j-1/2} + u^x_{i+1,j+1/2} \right), \tag{2.14}$$

$$(\mathcal{A}_x \tilde{D}_y \mu^x)_{i,j+1/2} = \frac{1}{2} \left(\tilde{D}_y \mu^x_{i-1/2,j+1/2} + \tilde{D}_y \mu^x_{i+1/2,j+1/2} \right), \tag{2.15}$$

$$\mathcal{A}_x d^y_{i,j+1/2} = \frac{1}{2} \left(d^y_{i-1/2,j+1/2} + d^y_{i+1/2,j+1/2} \right), \tag{2.16}$$

$$(\mathcal{A}_x \tilde{D}_y u^x)_{i+1/2,j+1/2} = \frac{1}{2} \left(\tilde{D}_y u^x_{i,j+1/2} + \tilde{D}_y u^x_{i+1,j+1/2} \right). \tag{2.17}$$

A few other average terms, such as $\mathcal{A}_{xy} u^y_{i,j+1/2}$, $(\mathcal{A}_y \tilde{D}_x \mu^y)_{i+1/2,j}$, $\mathcal{A}_x d^x_{i,j+1/2}$, $\mathcal{A}_y d^x_{i+1/2,j}$, $\mathcal{A}_y d^y_{i+1/2,j}$, $(\mathcal{A}_x \tilde{D}_y(\mu^x d^y)_{i,j+1/2}$, $(\mathcal{A}_y \tilde{D}_x \mu^y d^x)_{i+1/2,j}$, $(\mathcal{A}_x \tilde{D}_y(\mu^y d^x)_{i,j+1/2}$, $(\mathcal{A}_y \tilde{D}_x \mu^x d^y)_{i+1/2,j}$, $(\mathcal{A}_y \tilde{D}_x u^y)_{i+1/2,j+1/2}$, could be defined in the same manner.

2.2. The fully discrete numerical scheme and some further notation. Regarding the temporal approximation, we consider the following convex splitting treatment for the chemical potential vector:

$$\boldsymbol{\mu}^{n+1} = (\mu_1^{n+1}, \mu_2^{n+1})^T = \varepsilon^{-2}(|\boldsymbol{d}^{n+1}|^2 \boldsymbol{d}^{n+1} - \boldsymbol{d}^n) - \Delta \boldsymbol{d}^{n+1}, \tag{2.18}$$

with

$$\mu_i^{n+1} = \varepsilon^{-2}(|\boldsymbol{d}^{n+1}|^2 d_i^{n+1} - d_i^n) - \Delta d_i^{n+1}, \quad i = 1, 2. \tag{2.19}$$

The fully discrete scheme for the PDE system is formulated, with finite difference approximation in space:

$$\frac{\overline{\boldsymbol{u}}^{n+1} - \boldsymbol{u}^n}{\Delta t} + \frac{1}{2}(\boldsymbol{u}^n \cdot \nabla_h \overline{\boldsymbol{u}}^{n+1} + \nabla_h \cdot (\overline{\boldsymbol{u}}^{n+1}(\boldsymbol{u}^n)^T)) + \nabla_h p^n - \nu \Delta_h \overline{\boldsymbol{u}}^{n+1}$$
$$+ \lambda(\nabla_h \boldsymbol{\mu}^{n+1})^T \boldsymbol{d}^n + \lambda \nabla_h \cdot \left(\beta \boldsymbol{\mu}^{n+1}(\boldsymbol{d}^n)^T + (\beta+1)\boldsymbol{d}^n(\boldsymbol{\mu}^{n+1})^T \right) = 0, \tag{2.20}$$

$$\frac{\boldsymbol{u}^{n+1} - \overline{\boldsymbol{u}}^{n+1}}{\Delta t} + \nabla_h (p^{n+1} - p^n) = 0, \tag{2.21}$$

$$\nabla_h \cdot \boldsymbol{u}^{n+1} = 0, \tag{2.22}$$

$$\frac{\boldsymbol{d}^{n+1} - \boldsymbol{d}^n}{\Delta t} + \nabla_h \cdot (\boldsymbol{d}^n (\overline{\boldsymbol{u}}^{n+1})^T) + (\beta \nabla_h \overline{\boldsymbol{u}}^{n+1} + (1+\beta)(\nabla_h \overline{\boldsymbol{u}}^{n+1})^T) \boldsymbol{d}^n = -\gamma \boldsymbol{\mu}^{n+1}, \tag{2.23}$$

$$\varepsilon^{-2} (|\boldsymbol{d}^{n+1}|^2 \boldsymbol{d}^{n+1} - \boldsymbol{d}^n) - \Delta_h \boldsymbol{d}^{n+1} - \boldsymbol{\mu}^{n+1} = 0, \tag{2.24}$$

with the following discrete boundary conditions:

$$\left. (\overline{\boldsymbol{u}}^{n+1} \cdot \boldsymbol{n}) \right|_{\partial\Omega} = \left. (\boldsymbol{d}^{n+1} \cdot \boldsymbol{n}) \right|_{\partial\Omega} = \left. (\boldsymbol{u}^{n+1} \cdot \boldsymbol{n}) \right|_{\partial\Omega} = 0, \tag{2.25}$$

$$\left. (\boldsymbol{n} \cdot \nabla_h (\overline{\boldsymbol{u}}^{n+1} \cdot \tau)) \right|_{\partial\Omega} = \left. (\boldsymbol{n} \cdot \nabla_h (\boldsymbol{d}^{n+1} \cdot \tau)) \right|_{\partial\Omega} = 0. \tag{2.26}$$

For the initial data, $\boldsymbol{u}^0$, $\boldsymbol{d}^0$ are given, so that the initial chemical potential vector could be computed as $\boldsymbol{\mu}^0 = \varepsilon^{-2} (|\boldsymbol{d}^0|^2 \boldsymbol{d}^0 - \boldsymbol{d}^0) - \Delta_h \boldsymbol{d}^0$, and the initial data for the pressure field could be obtained through the following pressure Poisson equation

$$\begin{aligned}
-\Delta_h p^0 = \nabla_h \cdot \Big(&\frac{1}{2} (\boldsymbol{u}^0 \cdot \nabla_h \boldsymbol{u}^0 + \nabla_h \cdot (\boldsymbol{u}^0 (\boldsymbol{u}^0)^T)) \\
&+ \lambda (\nabla_h \boldsymbol{\mu}^0)^T \boldsymbol{d}^0 + \lambda \nabla_h \cdot \Big(\beta \boldsymbol{\mu}^0 (\boldsymbol{d}^0)^T + (\beta+1) \boldsymbol{d}^0 (\boldsymbol{\mu}^0)^T \Big) \Big),
\end{aligned} \tag{2.27}$$

$$\left. (\boldsymbol{n} \cdot \nabla_h p^0) \right|_{\partial\Omega} = 0.$$

REMARK 2.1.   An intermediate velocity vector $\overline{\boldsymbol{u}}^{n+1}$ is introduced in the numerical scheme (2.20)-(2.23). The advantage of this numerical approach could be observed from the fact that the Stokes solver is decoupled from the convection-diffusion part, since the pressure gradient is explicitly updated. This feature would greatly improve the numerical efficiency in the practical computation. In turn, the intermediate velocity vector $\overline{\boldsymbol{u}}^{n+1}$ and the orientation vector $\boldsymbol{d}^{n+1}$ form a closed system in (2.20), (2.23), as will be explained in the unique solvability analysis in the next subsection. Afterward, (2.21) and (2.22) stand for a standard Helmholtz projection of $\overline{\boldsymbol{u}}^{n+1}$ into the divergence-free space, at a discrete level. This projection is equivalent to a discrete Poisson equation, which could be very efficiently implemented.

DEFINITION 2.1.   *For any pair of variables u^a, u^b which are evaluated at the mesh points $(i, j+1/2)$, (such as u, $D_x \boldsymbol{d}$, $D_x \boldsymbol{\mu}$, $D_x p$, et cetera.), the discrete L_h^2-inner product is defined by*

$$\langle u^a, u^b \rangle_A = h^2 \sum_{j=0}^{N-1} \sum_{i=0}^{N} \gamma_i^{(0)} u_{i,j+1/2}^a u_{i,j+1/2}^b; \quad \gamma_i^{(0)} = \begin{cases} \frac{1}{2}, & \text{if } i=0 \text{ or } i=N, \\ 1, & \text{otherwise}, \end{cases} \tag{2.28}$$

for any pair of variables v^a, v^b which are evaluated at the mesh points $(i+1/2, j+1/2)$, (such as v, $D_y \boldsymbol{d}$, $D_y \boldsymbol{\mu}$, $D_y p$, et cetera.), the discrete L_h^2-inner product is defined by

$$\langle v^a, v^b \rangle_B = h^2 \sum_{j=0}^{N} \sum_{i=0}^{N-1} \gamma_j^{(1)} v_{i+1/2,j}^a v_{i+1/2,j}^b; \quad \gamma_j^{(1)} = \begin{cases} \frac{1}{2}, & \text{if } j=0 \text{ or } j=N, \\ 1, & \text{otherwise}, \end{cases} \tag{2.29}$$

for any pair of variables μ^a, μ^b which are evaluated at the mesh points $(i+1/2, j+1/2)$, (such as $\boldsymbol{\mu}$, $\boldsymbol{d}$, p, et cetera.), the discrete L_h^2-inner product is defined by

$$\langle \mu^a, \mu^b \rangle_C = h^2 \sum_{j=0}^{N-1} \sum_{i=0}^{N-1} \mu_{i+1/2,j+1/2}^a \mu_{i+1/2,j+1/2}^b. \tag{2.30}$$

In addition, for two velocity vectors $\boldsymbol{u} = (u^x, u^y)^T$ and $\boldsymbol{v} = (v^x, v^y)^T$, we denote their vector inner product as

$$\langle \boldsymbol{u}, \boldsymbol{v} \rangle_1 = \langle u^x, v^x \rangle_A + \langle u^y, v^y \rangle_B. \tag{2.31}$$

Their L_h^2 norms, namely, $\|\cdot\|_2$ norm, can be defined accordingly. Clearly all the discrete L_h^2 inner products defined above are second order accurate. In addition to the standard L_h^2 norm, we also introduce the L_h^p, $1 \le p < \infty$, and L_h^∞ norms for a grid function $f \in \mathcal{G}_N$:

$$\|f\|_\infty := \max_{i,j} |f_{i+1/2, j+1/2}|, \qquad \|f\|_p := \left(h^2 \sum_{i,j=0}^{N-1} |f_{i+1/2, j+1/2}|^p \right)^{\frac{1}{p}}, \quad 1 \le p < \infty. \tag{2.32}$$

The following summation by parts formulas will be useful in the later analysis.

LEMMA 2.1.   For discrete grid functions $\boldsymbol{u}$ (evaluated at $(x_i, y_{j+1/2})$), $\boldsymbol{v}$ (evaluated at $(x_{i+1/2}, y_j)$), $\boldsymbol{\mu}$, p, $\boldsymbol{d}$ (evaluated at $(x_{i+1/2}, y_{j+1/2})$) satisfying the discrete boundary conditions

$$(\boldsymbol{u} \cdot \boldsymbol{n})|_{\partial\Omega} = (\boldsymbol{v} \cdot \boldsymbol{n})|_{\partial\Omega} = (\boldsymbol{d} \cdot \boldsymbol{n})|_{\partial\Omega} = 0, \quad (\boldsymbol{n} \cdot \nabla_h(\boldsymbol{v} \cdot \boldsymbol{\tau}))|_{\partial\Omega} = (\boldsymbol{n} \cdot \nabla_h(\boldsymbol{d} \cdot \boldsymbol{\tau}))|_{\partial\Omega} = 0, \tag{2.33}$$

the following identities are valid:

$$\langle \boldsymbol{v}, \boldsymbol{u} \cdot \nabla_h \boldsymbol{v} \rangle_1 + \langle \boldsymbol{v}, \nabla_h \cdot (\boldsymbol{v} \boldsymbol{u}^T) \rangle_1 = 0, \tag{2.34}$$

$$\langle \boldsymbol{u}, \nabla_h p \rangle_1 = 0, \quad \text{if } \nabla_h \cdot \boldsymbol{u} = 0, \text{ and } (\boldsymbol{n} \cdot \boldsymbol{u})|_{\partial\Omega} = 0, \tag{2.35}$$

$$-\langle \boldsymbol{v}, \Delta_h \boldsymbol{v} \rangle_1 = \|\nabla_h \boldsymbol{v}\|_2^2 := \|\nabla_h v^x\|_1^2 + \|\nabla_h v^y\|_2^2, \tag{2.36}$$

$$\langle \boldsymbol{v}, (\nabla_h \boldsymbol{\mu})^T \boldsymbol{d} \rangle_1 = -\langle \boldsymbol{\mu}, \nabla_h \cdot (\boldsymbol{d} \boldsymbol{v}^T) \rangle_C, \tag{2.37}$$

$$\langle \boldsymbol{v}, \nabla_h \cdot (\boldsymbol{\mu} \boldsymbol{d}^T) \rangle_1 = -\langle \boldsymbol{\mu}, (\nabla_h \boldsymbol{v}) \boldsymbol{d} \rangle_C, \tag{2.38}$$

$$\langle \boldsymbol{v}, \nabla_h \cdot (\boldsymbol{d} \boldsymbol{\mu}^T) \rangle_1 = -\langle \boldsymbol{\mu}, (\nabla_h \boldsymbol{v})^T \boldsymbol{d} \rangle_C. \tag{2.39}$$

For any discrete grid function $\boldsymbol{d}$, the discrete version of the energy is defined as

$$E_h(\boldsymbol{d}) := \varepsilon^{-2} \left(\frac{1}{4} \|\boldsymbol{d}\|_4^4 - \frac{1}{2} \|\boldsymbol{d}\|_2^2 \right) + \frac{1}{2} \|\nabla_h \boldsymbol{d}\|_2^2. \tag{2.40}$$

2.3. Unique solvability analysis.   We implicitly define a linear operator $\mathcal{L}_h$ as follows. Assume that the fields $\boldsymbol{u}^n$, $\boldsymbol{d}^n$, and p^n are fixed. For each vector $\boldsymbol{\mu}$, $\boldsymbol{v} = \mathcal{L}_h \boldsymbol{\mu}$ is the unique solution of the following convection-diffusion equation:

$$\frac{\boldsymbol{v} - \boldsymbol{u}^n}{\Delta t} + \frac{1}{2}(\boldsymbol{u}^n \cdot \nabla_h \boldsymbol{v} + \nabla_h \cdot (\boldsymbol{v}(\boldsymbol{u}^n)^T)) + \nabla_h p^n - \nu \Delta_h \boldsymbol{v}$$
$$+ \lambda(\nabla_h \boldsymbol{\mu})^T \boldsymbol{d}^n + \lambda \nabla_h \cdot \left(\beta \boldsymbol{\mu}(\boldsymbol{d}^n)^T + (\beta+1) \boldsymbol{d}^n \boldsymbol{\mu}^T \right) = 0. \tag{2.41}$$

Thus, given the time level t^n and fields $(\boldsymbol{u}^n, \boldsymbol{d}^n, p^n)$, we can write $\overline{\boldsymbol{u}}^{n+1} = \mathcal{L}_h(\boldsymbol{\mu}^{n+1})$. In turn, $\boldsymbol{u}^{n+1}$ becomes the discrete Helmholtz projection of $\overline{\boldsymbol{u}}^{n+1}$ into divergence-free space, which we express as $\boldsymbol{u}^{n+1} = \mathcal{P}_h \overline{\boldsymbol{u}}^{n+1}$. Subsequently, a substitution of $\overline{\boldsymbol{u}}^{n+1} = \mathcal{L}_h(\boldsymbol{\mu}^{n+1})$ into (2.23) leads to the following system of equations for $\boldsymbol{d}^{n+1}$ and $\boldsymbol{\mu}^{n+1}$:

$$\frac{\boldsymbol{d}^{n+1} - \boldsymbol{d}^n}{\Delta t} = -\nabla_h \cdot (\boldsymbol{d}^n(\mathcal{L}_h(\boldsymbol{\mu}^{n+1}))^T) - (\beta \nabla_h(\mathcal{L}_h(\boldsymbol{\mu}^{n+1})) - (1+\beta)(\nabla_h(\mathcal{L}_h(\boldsymbol{\mu}^{n+1})))^T) \boldsymbol{d}^n$$

$$-\gamma\boldsymbol{\mu}^{n+1}, \tag{2.42}$$

$$\boldsymbol{\mu}^{n+1} = \varepsilon^{-2}(|\boldsymbol{d}^{n+1}|^2\boldsymbol{d}^{n+1} - \boldsymbol{d}^n) - \Delta_h\boldsymbol{d}^{n+1}. \tag{2.43}$$

We now rewrite (2.42) as

$$\frac{\boldsymbol{d}^{n+1} - \boldsymbol{d}^n}{\Delta t} = -\mathcal{G}_h(\boldsymbol{\mu}^{n+1}), \tag{2.44}$$

$$\mathcal{G}_h(\boldsymbol{\mu}) := \nabla_h \cdot (\boldsymbol{d}^n(\mathcal{L}_h\boldsymbol{\mu})^T) + (\beta\nabla_h(\mathcal{L}_h\boldsymbol{\mu}) + (1+\beta)(\nabla_h(\mathcal{L}_h\boldsymbol{\mu}))^T)\boldsymbol{d}^n + \gamma\boldsymbol{\mu}. \tag{2.45}$$

Notice that $\mathcal{G}_h : (\mathbb{R}^{N^2})^2 \to (\mathbb{R}^{N^2})^2$ is a linear operator (with the discrete boundary condition imposed). Furthermore, this linear operator is invertible, as demonstrated by the following lemma.

LEMMA 2.2.   *The linear operator $\mathcal{G}_h$ satisfies the monotonicity condition:*

$$\langle\mathcal{G}_h(\boldsymbol{\mu}^{(1)}) - \mathcal{G}_h(\boldsymbol{\mu}^{(2)}), \boldsymbol{\mu}^{(1)} - \boldsymbol{\mu}^{(2)}\rangle_C \geq \gamma\|\boldsymbol{\mu}^{(1)} - \boldsymbol{\mu}^{(2)}\|_2^2 \geq 0, \tag{2.46}$$

for any $\boldsymbol{\mu}^{(1)}$, $\boldsymbol{\mu}^{(2)}$. In addition, equality is realized if and only if $\boldsymbol{\mu}^{(1)} = \boldsymbol{\mu}^{(2)}$. Therefore, the operator $\mathcal{G}_h$ is invertible.

Proof.   We define the difference $\tilde{\boldsymbol{\mu}} := \boldsymbol{\mu}^{(1)} - \boldsymbol{\mu}^{(2)}$. Since $\mathcal{G}_h$ is a linear operator, we have

$$\begin{aligned}
&\mathcal{G}_h(\boldsymbol{\mu}^{(1)}) - \mathcal{G}_h(\boldsymbol{\mu}^{(2)}) \\
&= \mathcal{G}_h(\tilde{\boldsymbol{\mu}}) \\
&= \nabla_h \cdot (\boldsymbol{d}^n(\mathcal{L}_h\tilde{\boldsymbol{\mu}})^T) + (\beta\nabla_h(\mathcal{L}_h\tilde{\boldsymbol{\mu}}) + (1+\beta)(\nabla_h(\mathcal{L}_h\tilde{\boldsymbol{\mu}}))^T)\boldsymbol{d}^n + \gamma\tilde{\boldsymbol{\mu}}.
\end{aligned} \tag{2.47}$$

In turn, taking a discrete inner product with (2.47) by $\tilde{\boldsymbol{\mu}}$ yields

$$\begin{aligned}
\langle\mathcal{G}_h(\tilde{\boldsymbol{\mu}}), \tilde{\boldsymbol{\mu}}\rangle_C = &-\langle(\nabla_h\tilde{\boldsymbol{\mu}})^T\boldsymbol{d}^n, \mathcal{L}_h\tilde{\boldsymbol{\mu}}\rangle_1 - \beta\langle\tilde{\boldsymbol{\mu}}, \nabla_h(\mathcal{L}_h\tilde{\boldsymbol{\mu}})\boldsymbol{d}^n\rangle_C \\
&- (1+\beta)\langle\tilde{\boldsymbol{\mu}}, (\nabla_h(\mathcal{L}_h\tilde{\boldsymbol{\mu}})^T\boldsymbol{d}^n\rangle_C + \gamma\|\tilde{\boldsymbol{\mu}}\|_2^2.
\end{aligned} \tag{2.48}$$

Meanwhile, we define $\boldsymbol{v}^{(i)} := \mathcal{L}_h(\mu^{(i)})$, $i = 1, 2$, and $\tilde{\boldsymbol{v}} := \boldsymbol{v}^{(1)} - \boldsymbol{v}^{(2)} = \mathcal{L}_h\tilde{\boldsymbol{\mu}}$, using the linearity of $\mathcal{L}_h$. In addition, the definition of $\mathcal{L}_h$ in (2.41) implies that

$$\begin{aligned}
&\frac{\tilde{\boldsymbol{v}}}{\Delta t} + \frac{1}{2}(\boldsymbol{u}^n \cdot \nabla_h\tilde{\boldsymbol{v}} + \nabla_h \cdot (\tilde{\boldsymbol{v}}(\boldsymbol{u}^n)^T)) - \nu\Delta_h\tilde{\boldsymbol{v}} + \lambda(\nabla_h\tilde{\boldsymbol{\mu}})^T\boldsymbol{d}^n \\
&+ \lambda\nabla_h \cdot \left(\beta\tilde{\boldsymbol{\mu}}(\boldsymbol{d}^n)^T + (\beta+1)\boldsymbol{d}^n\tilde{\boldsymbol{\mu}}^T\right) = 0.
\end{aligned} \tag{2.49}$$

In turn, taking a discrete inner product with (2.49) by $\tilde{\boldsymbol{v}} = \mathcal{L}_h\tilde{\boldsymbol{\mu}}$ leads to

$$\begin{aligned}
&\frac{1}{\Delta t}\|\tilde{\boldsymbol{v}}\|_2^2 + \nu\|\nabla_h\tilde{\boldsymbol{v}}\|_2^2 + \lambda\langle(\nabla_h\tilde{\boldsymbol{\mu}})^T\boldsymbol{d}^n, \mathcal{L}_h\tilde{\boldsymbol{\mu}}\rangle_1 + \lambda\beta\langle\tilde{\boldsymbol{\mu}}, \nabla_h(\mathcal{L}_h\tilde{\boldsymbol{\mu}})\boldsymbol{d}^n\rangle_C \\
&+ \lambda(1+\beta)\langle\tilde{\boldsymbol{\mu}}, (\nabla_h(\mathcal{L}_h\tilde{\boldsymbol{\mu}})^T\boldsymbol{d}^n\rangle_C = 0,
\end{aligned} \tag{2.50}$$

in which we have made use of the following identities:

$$\langle\boldsymbol{u}^n \cdot \nabla_h\tilde{\boldsymbol{v}} + \nabla_h \cdot (\tilde{\boldsymbol{v}}(\boldsymbol{u}^n)^T), \tilde{\boldsymbol{v}}\rangle_1 = 0, \tag{2.51}$$

which follows the summation by parts formula, and

$$-(\tilde{\boldsymbol{v}}, \Delta_h\tilde{\boldsymbol{v}}) = \|\nabla_h\tilde{\boldsymbol{v}}\|_2^2. \tag{2.52}$$

As a consequence of (2.50), we get

$$\frac{1}{\lambda}\Big(\frac{1}{\Delta t}\|\tilde{\boldsymbol{v}}\|_2^2 + \nu\|\nabla_h\tilde{\boldsymbol{v}}\|_2^2\Big) = -\langle(\nabla_h\tilde{\boldsymbol{\mu}})^T\boldsymbol{d}^n, \mathcal{L}_h\tilde{\boldsymbol{\mu}}\rangle_1 - \beta\langle\tilde{\boldsymbol{\mu}}, \nabla_h(\mathcal{L}_h\tilde{\boldsymbol{\mu}})\boldsymbol{d}^n\rangle_C$$
$$- (1+\beta)\langle\tilde{\boldsymbol{\mu}}, (\nabla_h(\mathcal{L}_h\tilde{\boldsymbol{\mu}})^T\boldsymbol{d}^n\rangle_C. \tag{2.53}$$

Substitution of (2.53) into (2.48) yields

$$\langle\mathcal{G}_h(\tilde{\boldsymbol{\mu}}), \tilde{\boldsymbol{\mu}}\rangle_C = \frac{1}{\lambda}\Big(\frac{1}{\Delta t}\|\tilde{\boldsymbol{v}}\|_2^2 + \nu\|\nabla_h\tilde{\boldsymbol{v}}\|_2^2\Big) + \gamma\|\tilde{\boldsymbol{\mu}}\|_2^2. \tag{2.54}$$

This is equivalent to

$$\langle\mathcal{G}_h(\boldsymbol{\mu}^{(1)}) - \mathcal{G}_h(\boldsymbol{\mu}^{(2)}), \boldsymbol{\mu}^{(1)} - \boldsymbol{\mu}^{(2)}\rangle_C = \langle\mathcal{G}_h(\tilde{\boldsymbol{\mu}}), \tilde{\boldsymbol{\mu}}\rangle_C$$
$$\geq \gamma\|\tilde{\boldsymbol{\mu}}\|_2^2$$
$$= \gamma\|\boldsymbol{\mu}^{(1)} - \boldsymbol{\mu}^{(2)}\|_2^2$$
$$\geq 0, \tag{2.55}$$

so that (2.46) has been proved. In addition, it is clear that equality is valid if and only if $\tilde{\boldsymbol{\mu}} \equiv 0$, i.e., $\boldsymbol{\mu}^{(1)} = \boldsymbol{\mu}^{(2)}$. The proof is complete.   □

REMARK 2.2.   The standard monotonicity condition for a linear operator $\mathcal{G}_h$ is given by $(\mathcal{G}_h(\boldsymbol{\mu}), \boldsymbol{\mu}) \geq 0$. On the other hand, since two non-homogeneous terms have been involved in the definition (2.41) of $\mathcal{L}_h\mu$, namely $\frac{\boldsymbol{u}^n}{\Delta t}$ and $\nabla_h p^n$, such a monotonicity condition is not precise. To avoid this non-homogeneous issue, we use an alternate monotonicity condition, $(\mathcal{G}_h(\boldsymbol{\mu}^2) - \mathcal{G}_h(\boldsymbol{\mu}^1), \boldsymbol{\mu}^2 - \boldsymbol{\mu}^1) \geq 0$, which turns out to be more precise.

Since the linear operator $\mathcal{G}_h$ maps $(\mathbb{R}^{N^2})^2$ into $(\mathbb{R}^{N^2})^2$, we see that the inverse operator $\mathcal{G}_h^{-1}$ also maps $(\mathbb{R}^{N^2})^2$ into $(\mathbb{R}^{N^2})^2$. As a direct consequence of Lemma 2.2, the following result is available.

COROLLARY 2.1.   *The linear operator $\mathcal{G}_h^{-1}$ also satisfies the monotonicity condition:*

$$\langle\mathcal{G}_h^{-1}(\boldsymbol{d}^{(1)}) - \mathcal{G}_h^{-1}(\boldsymbol{d}^{(2)}), \boldsymbol{d}^{(1)} - \boldsymbol{d}^{(2)}\rangle_C \geq \gamma\|\mathcal{G}_h^{-1}(\boldsymbol{d}^{(1)} - \boldsymbol{d}^{(2)})\|_2^2 \geq 0, \tag{2.56}$$

for any $\boldsymbol{d}^{(1)}$, $\boldsymbol{d}^{(2)}$. In addition, the equality is valid if and only if $\boldsymbol{d}^{(1)} = \boldsymbol{d}^{(2)}$.

Proof.   We denote $\boldsymbol{\mu}^{(i)} = \mathcal{G}_h^{-1}(\boldsymbol{d}^{(i)})$, $i = 1, 2$, which is equivalent to $\boldsymbol{d}^{(i)} = \mathcal{G}_h\boldsymbol{\mu}^{(i)}$, $i = 1, 2$. An application of (2.46) reveals that

$$\langle\mathcal{G}_h^{-1}(\boldsymbol{d}^{(1)}) - \mathcal{G}_h^{-1}(\boldsymbol{d}^{(2)}), \boldsymbol{d}^{(1)} - \boldsymbol{d}^{(2)}\rangle_C = \langle\mathcal{G}_h(\boldsymbol{\mu}^{(1)}) - \mathcal{G}_h(\boldsymbol{\mu}^{(2)}), \boldsymbol{\mu}^{(1)} - \boldsymbol{\mu}^{(2)}\rangle_C$$
$$\geq \gamma\|\boldsymbol{\mu}^{(1)} - \boldsymbol{\mu}^{(2)}\|_2^2$$
$$= \gamma\|\mathcal{G}_h^{-1}(\boldsymbol{d}^{(1)} - \boldsymbol{d}^{(2)})\|_2^2$$
$$\geq 0. \tag{2.57}$$

Clearly, the equality is valid if and only if $\boldsymbol{d}^{(1)} = \boldsymbol{d}^{(2)}$. This finishes the proof for Corollary 2.1.   □

The Browder-Minty lemma is needed in the unique solvability analysis.

LEMMA 2.3 (Browder-Minty [4, 42]).   *Let X be a real, reflexive Banach space and suppose X' is its dual. Let $T : X \to X'$ be (i) bounded; (ii) continuous; (iii) coercive, that is,*

$$\frac{\langle T(u), u\rangle}{\|u\|_X} \to +\infty \quad as \quad \|u\|_X \to +\infty; \tag{2.58}$$

and (iv) monotone. Then for any $g \in X'$ there exists a solution $u \in X$ of the equation $T(u) = g$. Furthermore, if the operator T is strictly monotone, then the solution u is unique.

Then we proceed into the proof of unique solvability.

THEOREM 2.1. *Given $\boldsymbol{u}^n$, $\boldsymbol{d}^n$, and p^n, the proposed numerical scheme* (2.20)-(2.23) *is unconditionally uniquely solvable.*

Proof. By (2.44)-(2.45), we have an alternate representation $\boldsymbol{\mu}^{n+1} = -\mathcal{G}_h^{-1}(\frac{\boldsymbol{d}^{n+1}-\boldsymbol{d}^n}{\Delta t})$. Meanwhile, with the formula (2.43), the numerical scheme (2.20)-(2.23) is equivalent to

$$\mathcal{G}_h^{-1}(\frac{\boldsymbol{d}^{n+1}-\boldsymbol{d}^n}{\Delta t}) + \varepsilon^{-2}(|\boldsymbol{d}^{n+1}|^2\boldsymbol{d}^{n+1} - \boldsymbol{d}^n) - \Delta_h \boldsymbol{d}^{n+1} = 0, \tag{2.59}$$

which becomes a closed system for $\boldsymbol{d}^{n+1}$. In other words, the numerical solution (2.20)-(2.23) is equivalent to the following nonlinear system:

$$\mathcal{F}_h(\boldsymbol{d}) := \mathcal{G}_h^{-1}(\frac{\boldsymbol{d}-\boldsymbol{d}^n}{\Delta t}) + \varepsilon^{-2}(|\boldsymbol{d}|^2\boldsymbol{d} - \boldsymbol{d}^n) - \Delta_h \boldsymbol{d} = 0. \tag{2.60}$$

It is clear that $\mathcal{F}_h$ maps $(\mathbb{R}^{N^2})^2$ into $(\mathbb{R}^{N^2})^2$, with the imposed discrete boundary conditions. In turn, we set $X = X' = (\mathbb{R}^{N^2})^2$, equipped with the discrete $\|\cdot\|_2$ norm: $\|\boldsymbol{f}\|_X = \|\boldsymbol{f}\|_2$, for any $(\mathbb{R}^{N^2})^2$ with the imposed discrete boundary conditions. Next, we prove its continuity in the $\|\cdot\|_2$ norm, with fixed values of Δt and h. Consider $\boldsymbol{d}^{(0)}, \boldsymbol{d}^{(1)} \in (\mathbb{R}^{N^2})^2$, satisfying the imposed discrete boundary conditions, with $\|\boldsymbol{d}^{(1)} - \boldsymbol{d}^{(0)}\|_2 = \delta$. In turn, we denote $\boldsymbol{\mu}^{(i)} = \mathcal{G}_h^{-1}(\frac{\boldsymbol{d}^{(i)}-\boldsymbol{d}^n}{\Delta t})$, $i = 0, 1$, respectively. By the monotonicity estimate (2.56) (in Corollary 2.1), we see that

$$\left\langle \boldsymbol{\mu}^{(0)} - \boldsymbol{\mu}^{(1)}, \frac{\boldsymbol{d}^{(0)}-\boldsymbol{d}^n}{\Delta t} - \frac{\boldsymbol{d}^{(1)}-\boldsymbol{d}^n}{\Delta t} \right\rangle_C \geq \gamma \|\boldsymbol{\mu}^{(0)} - \boldsymbol{\mu}^{(1)}\|_2^2,$$

so that

$$\frac{\gamma}{2}\|\boldsymbol{\mu}^{(0)} - \boldsymbol{\mu}^{(1)}\|_2^2 + \frac{1}{2\gamma\Delta t^2}\|\boldsymbol{d}^{(0)} - \boldsymbol{d}^{(1)}\|_2^2 \geq \gamma \|\boldsymbol{\mu}^{(0)} - \boldsymbol{\mu}^{(1)}\|_2^2, \tag{2.61}$$

which, in turn, leads to

$$\|\boldsymbol{\mu}^{(0)} - \boldsymbol{\mu}^{(1)}\|_2^2 \leq \frac{1}{\gamma^2\Delta t^2}\|\boldsymbol{d}^{(0)} - \boldsymbol{d}^{(1)}\|_2^2, \quad \|\boldsymbol{\mu}^{(0)} - \boldsymbol{\mu}^{(1)}\|_2 \leq \frac{1}{\gamma\Delta t}\|\boldsymbol{d}^{(0)} - \boldsymbol{d}^{(1)}\|_2. \tag{2.62}$$

As a result, $\boldsymbol{\mu}^{(1)} \to \boldsymbol{\mu}^{(0)}$ as $\boldsymbol{d}^{(1)} \to \boldsymbol{d}^{(0)}$ in the discrete L_h^2 norm, for a fixed value of Δt. The continuity of $\mathcal{G}_h$ has been proved. The continuity analysis of the remaining two terms in the expression of $\mathcal{F}_h$ is more straightforward:

$$\begin{aligned}\varepsilon^{-2}\|(|\boldsymbol{d}^{(0)}|^2\boldsymbol{d}^{(0)} - |\boldsymbol{d}^{(1)}|^2\boldsymbol{d}^{(1)})\|_2 &\leq C\varepsilon^{-2}(\|\boldsymbol{d}^{(0)}\|_6^2 + \|\boldsymbol{d}^{(1)}\|_6^2)\|\boldsymbol{d}^{(0)} - \boldsymbol{d}^{(1)}\|_6) \\ &\leq C\varepsilon^{-2}h^{-3}(\|\boldsymbol{d}^{(0)}\|_2^2 + \|\boldsymbol{d}^{(1)}\|_2^2)\|\boldsymbol{d}^{(0)} - \boldsymbol{d}^{(1)}\|_2),\end{aligned} \tag{2.63}$$

and

$$\|\Delta_h \boldsymbol{d}^{(0)} - \Delta_h \boldsymbol{d}^{(1)}\|_2 \leq Ch^{-2}\|\boldsymbol{d}^{(0)} - \boldsymbol{d}^{(1)}\|_2, \tag{2.64}$$

where a discrete Hölder inequality has been applied in the first step of (2.63), and where the second step comes from a 3-D inverse inequality: $h\|f\|_6 \le C\|f\|_2$. Therefore, a combination of (2.62)-(2.63) reveals that, $\mathcal{F}_h(\boldsymbol{d}^{(1)}) \to \mathcal{F}_h(\boldsymbol{d}^{(0)})$ as $\boldsymbol{d}^{(1)} \to \boldsymbol{d}^{(0)}$ in the discrete L_h^2 norm, for fixed values of Δt and h. This finishes the continuity analysis of $\mathcal{F}_h$.

To establish the coercive property of $\mathcal{F}_h$, we begin with the following expansion:

$$\langle \mathcal{F}_h(\boldsymbol{d}), \boldsymbol{d} \rangle_C = \langle \mathcal{G}_h^{-1}(\frac{\boldsymbol{d}-\boldsymbol{d}^n}{\Delta t}), \boldsymbol{d} \rangle_C + \varepsilon^{-2} \langle (|\boldsymbol{d}|^2 \boldsymbol{d} - \boldsymbol{d}^n), \boldsymbol{d} \rangle_C + \langle -\Delta_h \boldsymbol{d}, \boldsymbol{d} \rangle_C$$
$$= \frac{1}{\Delta t}(\langle \mathcal{G}_h^{-1}(\boldsymbol{d}-\boldsymbol{d}^n), \boldsymbol{d}-\boldsymbol{d}^n \rangle_C + \langle \mathcal{G}_h^{-1}(\boldsymbol{d}-\boldsymbol{d}^n), \boldsymbol{d}^n \rangle_C)$$
$$+ \varepsilon^{-2}(\|\boldsymbol{d}\|_4^4 - \langle \boldsymbol{d}^n, \boldsymbol{d} \rangle_C) + \|\nabla_h \boldsymbol{d}\|_2^2, \tag{2.65}$$

with summation by parts formula applied. For the first part, we apply the monotonicity estimate (2.56) and obtain

$$\langle \mathcal{G}_h^{-1}(\boldsymbol{d}-\boldsymbol{d}^n), \boldsymbol{d}-\boldsymbol{d}^n \rangle_C \ge \gamma \|\mathcal{G}_h^{-1}(\boldsymbol{d}-\boldsymbol{d}^n)\|_2^2,$$
$$\langle \mathcal{G}_h^{-1}(\boldsymbol{d}-\boldsymbol{d}^n), \boldsymbol{d}^n \rangle_C \ge -\frac{\gamma}{2}\|\mathcal{G}_h^{-1}(\boldsymbol{d}-\boldsymbol{d}^n)\|_2^2 - \frac{1}{2\gamma}\|\boldsymbol{d}^n\|_2^2, \tag{2.66}$$

so that

$$\langle \mathcal{G}_h^{-1}(\boldsymbol{d}-\boldsymbol{d}^n), \boldsymbol{d}-\boldsymbol{d}^n \rangle_C + \langle \mathcal{G}_h^{-1}(\boldsymbol{d}-\boldsymbol{d}^n), \boldsymbol{d}^n \rangle_C \ge \frac{\gamma}{2}\|\mathcal{G}_h^{-1}(\boldsymbol{d}-\boldsymbol{d}^n)\|_2^2 - \frac{1}{2\gamma}\|\boldsymbol{d}^n\|_2^2. \tag{2.67}$$

For the second part of (2.65), we observe that an application of quadratic inequality reveals that

$$\|\boldsymbol{d}\|_4^4 \ge 2\|\boldsymbol{d}\|_2^2 - |\Omega|, \quad -\langle \boldsymbol{d}^n, \boldsymbol{d} \rangle_C \ge -\frac{1}{2}(\|\boldsymbol{d}\|_2^2 + \|\boldsymbol{d}^n\|_2^2), \tag{2.68}$$

so that

$$\|\boldsymbol{d}\|_4^4 - \langle \boldsymbol{d}^n, \boldsymbol{d} \rangle_C \ge \|\boldsymbol{d}\|_2^2 - \frac{1}{2}\|\boldsymbol{d}^n\|_2^2 - |\Omega|. \tag{2.69}$$

As a result, a substitution of (2.67)-(2.69) into (2.69) leads to the following estimate:

$$\frac{\langle \mathcal{F}_h(\boldsymbol{d}), \boldsymbol{d} \rangle_C}{\|\boldsymbol{d}\|_2} \ge \frac{\|\boldsymbol{d}\|_2^2 - (\frac{1}{2}+\frac{1}{2\gamma})\|\boldsymbol{d}^n\|_2^2 - |\Omega|}{\|\boldsymbol{d}\|_2} = \|\boldsymbol{d}\|_2 - \frac{Q^{(0)}}{\|\boldsymbol{d}\|_2} \to +\infty, \quad \text{as } \|\boldsymbol{d}\|_2 \to +\infty, \tag{2.70}$$

with $Q^{(0)} = (\frac{1}{2}+\frac{1}{2\gamma})\|\boldsymbol{d}^n\|_2^2 + |\Omega|$, a fixed constant. This finishes the coercive analysis of $\mathcal{F}_h$.

The remaining work is focused on establishing a monotonicity condition for the nonlinear operator $\mathcal{F}_h(\boldsymbol{d})$. Given $\boldsymbol{d}^{(1)}$, $\boldsymbol{d}^{(2)}$, we denote $\tilde{\boldsymbol{d}} = \boldsymbol{d}^{(1)} - \boldsymbol{d}^{(2)}$, and a direct calculation gives

$$\mathcal{F}_h(\boldsymbol{d}^{(1)}) - \mathcal{F}_h(\boldsymbol{d}^{(2)}) = \mathcal{G}_h^{-1}(\frac{\boldsymbol{d}^{(1)}-\boldsymbol{d}^{(2)}}{\Delta t}) + \varepsilon^{-2}(|\boldsymbol{d}^{(1)}|^2 \boldsymbol{d}^{(1)} - |\boldsymbol{d}^{(2)}|^2 \boldsymbol{d}^{(2)}) - \Delta_h \tilde{\boldsymbol{d}}. \tag{2.71}$$

In addition, the following estimates are available:

$$\left\langle \mathcal{G}_h^{-1}(\frac{\boldsymbol{d}^{(1)}-\boldsymbol{d}^{(2)}}{\Delta t}), \boldsymbol{d}^{(1)} - \boldsymbol{d}^{(2)} \right\rangle_C \ge 0, \tag{2.72}$$

$$\langle |\boldsymbol{d}^{(1)}|^2 \boldsymbol{d}^{(1)} - |\boldsymbol{d}^{(2)}|^2 \boldsymbol{d}^{(2)}, \boldsymbol{d}^{(1)} - \boldsymbol{d}^{(2)} \rangle_C \geq 0, \tag{2.73}$$

$$\langle -\Delta_h \tilde{\boldsymbol{d}}, \tilde{\boldsymbol{d}} \rangle_C = \|\nabla_h \tilde{\boldsymbol{d}}\|_2^2 \geq 0, \tag{2.74}$$

with equality in (2.72) and (2.73) iff $\boldsymbol{d}^{(1)} = \boldsymbol{d}^{(2)}$. Note that we have applied (2.57) to obtain (2.72). Then we arrive at

$$\langle \mathcal{F}_h(\boldsymbol{d}^{(1)}) - \mathcal{F}_h(\boldsymbol{d}^{(2)}), \boldsymbol{d}^{(1)} - \boldsymbol{d}^{(2)} \rangle_C \geq 0, \tag{2.75}$$

for any $\boldsymbol{d}^{(1)}$, $\boldsymbol{d}^{(2)}$, with equality iff $\boldsymbol{d}^{(1)} = \boldsymbol{d}^{(2)}$. Therefore, an application of the Browder-Minty lemma implies a unique solution for (2.60), so that the unique solvability of the numerical scheme (2.20)-(2.23) has been established. This finishes the proof of Theorem 2.1. □

3. Energy stability analysis

THEOREM 3.1. *Given $\boldsymbol{u}^n$, $\boldsymbol{d}^n$, p^n, and any $\Delta t > 0$, $h > 0$, let $\boldsymbol{u}^{n+1}$, d^{n+1}, and p^{n+1} be the unique solution triple of the proposed numerical scheme (2.20)-(2.23). The scheme is unconditionally energy stable in the sense that $\widetilde{E}_h(\boldsymbol{d}^{n+1}, \boldsymbol{u}^{n+1}, p^{n+1}) \leq \widetilde{E}_h(\boldsymbol{d}^n, \boldsymbol{u}^n, p^n)$, where*

$$\widetilde{E}_h(\boldsymbol{d}^n, \boldsymbol{u}^n, p^n) := \lambda E_h(\boldsymbol{d}^n) + \frac{1}{2}\|\boldsymbol{u}^n\|_2^2 + \frac{\Delta t^2}{2}\|\nabla_h p^n\|_2^2. \tag{3.1}$$

Proof. Taking a discrete inner product of (2.23) with $\boldsymbol{\mu}^{n+1}$ gives

$$\langle \boldsymbol{d}^{n+1} - \boldsymbol{d}^n, \boldsymbol{\mu}^{n+1} \rangle_C + \Delta t \gamma \|\boldsymbol{\mu}^{n+1}\|_2^2$$
$$= \Delta t \langle (\nabla_h \boldsymbol{\mu}^{n+1})^T \boldsymbol{d}^n, \overline{\boldsymbol{u}}^{n+1} \rangle_1 - \Delta t \beta \langle (\nabla_h \overline{\boldsymbol{u}}^{n+1}) \boldsymbol{d}^n, \boldsymbol{\mu}^{n+1} \rangle_C$$
$$- \Delta t (1+\beta) \langle (\nabla_h \overline{\boldsymbol{u}}^{n+1})^T \boldsymbol{d}^n, \boldsymbol{\mu}^{n+1} \rangle_C, \tag{3.2}$$

with repeated applications of summation by parts. Meanwhile, the convex splitting treatment of the vector chemical potential (2.18)-(2.19) implies that

$$\langle \boldsymbol{d}^{n+1} - \boldsymbol{d}^n, \boldsymbol{\mu}^{n+1} \rangle_C \geq E_h(\boldsymbol{d}^{n+1}) - E_h(\boldsymbol{d}^n), \tag{3.3}$$

which comes from the following energy inequalities:

$$\langle |\boldsymbol{d}^{n+1}|^2 \boldsymbol{d}^{n+1}, \boldsymbol{d}^{n+1} - \boldsymbol{d}^n \rangle_C \geq \frac{1}{4}(\|\boldsymbol{d}^{n+1}\|_4^4 - \|\boldsymbol{d}^n\|_4^4),$$

$$\langle -\boldsymbol{d}^n, \boldsymbol{d}^{n+1} - \boldsymbol{d}^n \rangle_C \geq -\frac{1}{2}(\|\boldsymbol{d}^{n+1}\|_2^2 - \|\boldsymbol{d}^n\|_2^2),$$

$$\langle -\Delta_h \boldsymbol{d}^{n+1}, \boldsymbol{d}^{n+1} - \boldsymbol{d}^n \rangle_C \geq \frac{1}{2}(\|\nabla_h \boldsymbol{d}^{n+1}\|_2^2 - \|\nabla_h \boldsymbol{d}^n\|_2^2). \tag{3.4}$$

Taking a discrete inner product with (2.20) by $\overline{\boldsymbol{u}}^{n+1}$ leads to

$$\frac{1}{2}(\|\overline{\boldsymbol{u}}^{n+1}\|_2^2 - \|\boldsymbol{u}^n\|_2^2 + \|\overline{\boldsymbol{u}}^{n+1} - \boldsymbol{u}^n\|_2^2) + \nu\|\nabla_h \overline{\boldsymbol{u}}^{n+1}\|_2^2 + \Delta t \langle \nabla_h p^n, \overline{\boldsymbol{u}}^{n+1} \rangle_1$$
$$= -\lambda \Delta t \langle (\nabla_h \boldsymbol{\mu}^{n+1})^T \boldsymbol{d}^n, \overline{\boldsymbol{u}}^{n+1} \rangle_1 + \lambda \beta \Delta t \langle (\nabla_h \overline{\boldsymbol{u}}^{n+1}) \boldsymbol{d}^n, \boldsymbol{\mu}^{n+1} \rangle_C$$
$$+ \lambda(1+\beta)\Delta t \langle (\nabla_h \overline{\boldsymbol{u}}^{n+1})^T \boldsymbol{d}^n, \boldsymbol{\mu}^{n+1} \rangle_C, \tag{3.5}$$

where the following identities have been used:

$$\langle \boldsymbol{u}^n \cdot \nabla_h \overline{\boldsymbol{u}}^{n+1} + \nabla_h \cdot (\overline{\boldsymbol{u}}^{n+1}(\boldsymbol{u}^n)^T), \overline{\boldsymbol{u}}^{n+1} \rangle_1 = 0, \qquad \text{(by summation-by-parts)} \tag{3.6}$$

$$\langle -\Delta_h \overline{\boldsymbol{u}}^{n+1}, \overline{\boldsymbol{u}}^{n+1} \rangle_1 = \|\nabla_h \overline{\boldsymbol{u}}^{n+1}\|_2^2. \tag{3.7}$$

Regarding the term $\langle \nabla_h p^n, \overline{\boldsymbol{u}}^{n+1} \rangle_1$, the following identity is available:

$$
\begin{aligned}
\langle \nabla_h p^n, \overline{\boldsymbol{u}}^{n+1} \rangle_1 &= -\langle p^n, \nabla_h \cdot \overline{\boldsymbol{u}}^{n+1} \rangle_C \\
&= -\langle p^n, \Delta t \Delta_h (p^{n+1} - p^n) \rangle_C \\
&= \Delta t \langle \nabla_h p^n, \nabla_h (p^{n+1} - p^n) \rangle_1 \\
&= \frac{\Delta t}{2} (\|\nabla_h p^{n+1}\|_2^2 - \|\nabla_h p^n\|_2^2) - \frac{\Delta t}{2} \|\nabla_h (p^{n+1} - p^n)\|_2^2 \\
&= \frac{\Delta t}{2} (\|\nabla_h p^{n+1}\|_2^2 - \|\nabla_h p^n\|_2^2) - \frac{1}{2\Delta t} \|\boldsymbol{u}^{n+1} - \overline{\boldsymbol{u}}^{n+1}\|_2^2, \tag{3.8}
\end{aligned}
$$

where (2.22) has been applied in the derivation. A substitution of (3.8) into (3.5) yields

$$
\begin{aligned}
&\frac{1}{2}(\|\overline{\boldsymbol{u}}^{n+1}\|_2^2 - \|\boldsymbol{u}^n\|_2^2 + \|\overline{\boldsymbol{u}}^{n+1} - \boldsymbol{u}^n\|_2^2) + \nu\|\nabla_h \overline{\boldsymbol{u}}^{n+1}\|_2^2 + \frac{\Delta t^2}{2}(\|\nabla_h p^{n+1}\|_2^2 - \|\nabla_h p^n\|_2^2) \\
&= \frac{1}{2}\|\boldsymbol{u}^{n+1} - \overline{\boldsymbol{u}}^{n+1}\|_2^2 - \lambda \Delta t \langle (\nabla_h \boldsymbol{\mu}^{n+1})\boldsymbol{d}^n, \overline{\boldsymbol{u}}^{n+1} \rangle_1 + \lambda \beta \Delta t \langle (\nabla_h \overline{\boldsymbol{u}}^{n+1})\boldsymbol{d}^n, \boldsymbol{\mu}^{n+1} \rangle_C \\
&\quad + \lambda(1+\beta)\Delta t \langle (\nabla_h \overline{\boldsymbol{u}}^{n+1})^T \boldsymbol{d}^n, \boldsymbol{\mu}^{n+1} \rangle_C. \tag{3.9}
\end{aligned}
$$

Taking a discrete inner product with (2.22) by $\boldsymbol{u}^{n+1}$ results in

$$\|\boldsymbol{u}^{n+1}\|_2^2 - \|\overline{\boldsymbol{u}}^{n+1}\|_2^2 + \|\boldsymbol{u}^{n+1} - \overline{\boldsymbol{u}}^{n+1}\|_2^2 = 0, \tag{3.10}$$

since $\langle \boldsymbol{u}^{n+1}, \nabla_h (p^{n+1} - p^n) \rangle_1 = 0$. A combination of the last identity with (3.9) reveals that

$$
\begin{aligned}
&\frac{1}{2}(\|\boldsymbol{u}^{n+1}\|_2^2 - \|\boldsymbol{u}^n\|_2^2) + \nu\|\nabla_h \overline{\boldsymbol{u}}^{n+1}\|_2^2 + \frac{\Delta t^2}{2}(\|\nabla_h p^{n+1}\|_2^2 - \|\nabla_h p^n\|_2^2) \\
&\leq -\lambda \Delta t \langle (\nabla_h \boldsymbol{\mu}^{n+1})^T \boldsymbol{d}^n, \overline{\boldsymbol{u}}^{n+1} \rangle_1 + \lambda \beta \Delta t \langle (\nabla_h \overline{\boldsymbol{u}}^{n+1})\boldsymbol{d}^n, \boldsymbol{\mu}^{n+1} \rangle_C \\
&\quad + \lambda(1+\beta)\Delta t \langle (\nabla_h \overline{\boldsymbol{u}}^{n+1})^T \boldsymbol{d}^n, \boldsymbol{\mu}^{n+1} \rangle_C. \tag{3.11}
\end{aligned}
$$

Finally, a combination of (3.2), (3.3) and (3.11) yields the desired stability result:

$$
\begin{aligned}
&\lambda(E_h(\boldsymbol{d}^{n+1}) - E_h(\boldsymbol{d}^n)) + \Delta t \gamma \|\boldsymbol{\mu}^{n+1}\|_2^2 + \frac{1}{2}(\|\boldsymbol{u}^{n+1}\|_2^2 - \|\boldsymbol{u}^n\|_2^2) \\
&\quad + \nu\|\nabla_h \overline{\boldsymbol{u}}^{n+1}\|_2^2 + \frac{\Delta t^2}{2}(\|\nabla_h p^{n+1}\|_2^2 - \|\nabla_h p^n\|_2^2) \leq 0, \tag{3.12}
\end{aligned}
$$

which in turn implies the desired unconditional energy stability result:

$$\lambda E_h(\boldsymbol{d}^{n+1}) + \frac{1}{2}\|\boldsymbol{u}^{n+1}\|_2^2 + \frac{\Delta t^2}{2}\|\nabla_h p^{n+1}\|_2^2 \leq \lambda E_h(\boldsymbol{d}^n) + \frac{1}{2}\|\boldsymbol{u}^n\|_2^2 + \frac{\Delta t^2}{2}\|\nabla_h p^n\|_2^2.$$

This completes the proof of the theorem. □

REMARK 3.1.   In the decomposition (3.1) for the modified energy functional $\widetilde{E}_h(\boldsymbol{d}^n, \boldsymbol{u}^n, p^n)$, we see that $\lambda E_h(\boldsymbol{d}^n)$ is the standard phase field energy, $\frac{1}{2}\|\boldsymbol{u}^n\|_2^2$ stands for the kinematic energy, and $\frac{\Delta t^2}{2}\|\nabla_h p^n\|_2^2$ turns out to be an additional correction term associated with the numerical scheme. In other words, the first two terms correspond to the physical energy in the continuous version (1.14), while the additional correction

term does not have any physical meaning; this additional correction term is of order $O(\Delta t^2)$, and it appears because of the decoupled treatment of the Stokes solver.

As a result of this energy stability, we are able to derive a uniform-in-time H_h^1, L_h^4 and L_h^6 bounds for the numerical solution, which will be extensively used in the convergence analysis. Before the statement of the desired result, we need the following discrete Sobolev inequality; its proof will be provided in the appendix.

LEMMA 3.1.   *For any grid function f, we have*

$$\|f\|_6 \leq C_1 \|f\|_{H_h^1}, \quad where \quad \|f\|_{H_h^1}^2 := \|f\|_2^2 + \|\nabla_h f\|_2^2, \tag{3.13}$$

$$\|f\|_4 \leq C_2 (\|f\|_2 + \|f\|_2^{\frac{1}{4}} \cdot \|\nabla_h f\|_2^{\frac{3}{4}}), \tag{3.14}$$

$$\|\nabla_h f\|_4 \leq C_2 \|\nabla_h f\|_2^{\frac{1}{4}} \cdot \|\Delta_h f\|_2^{\frac{3}{4}}, \tag{3.15}$$

$$\|f\|_\infty \leq C_3 (\|f\|_2 + \|\nabla_h f\|_2^{\frac{1}{2}} \cdot \|\Delta_h f\|_2^{\frac{1}{2}}), \tag{3.16}$$

with C_i only dependent on Ω, $1 \leq i \leq 3$.

COROLLARY 3.1.   *Given initial data $\boldsymbol{u}^0$, $\boldsymbol{d}^0$, and p^0, where p^0 is obtained by the discrete Poisson problem (2.27), the following H_h^1, L_h^4 and L_h^6 bounds for the numerical solution are available:*

$$\max_{1 \leq k \leq M} \|\boldsymbol{d}^k\|_{H_h^1} \leq M_0^{(1)}, \quad \max_{1 \leq k \leq M} \|\boldsymbol{d}^k\|_4 \leq M_0^{(4)}, \quad \max_{1 \leq k \leq M} \|\boldsymbol{d}^k\|_6 \leq M_0^{(6)}, \tag{3.17}$$

where $M_0^{(1)}$, $M_0^{(4)}$ and $M_0^{(6)}$ are time independent. Moreover, $M_0^{(4)}$ is ε-independent, $M_0^{(1)}$ and $M_0^{(6)}$ are order of $O(\varepsilon^{-1})$.

Proof.   By the energy stability estimate in Theorem 3.1, the following induction could be made:

$$E_h(\boldsymbol{d}^k) \leq \widetilde{E}_h(\boldsymbol{d}^k, \boldsymbol{u}^k, p^k) \leq \ldots \leq \widetilde{E}_h(\boldsymbol{d}^0, \boldsymbol{u}^0, p^0) := \tilde{M}_0, \quad \forall k \geq 0, \tag{3.18}$$

in which $\tilde{M}_0$ is of order $O(\varepsilon^{-2})$. In turn, by the definition (2.40), we get

$$\frac{1}{4} \|\boldsymbol{d}^k\|_4^4 - \frac{1}{2} \|\boldsymbol{d}^k\|_2^2 + \frac{\varepsilon^2}{2} \|\nabla_h \boldsymbol{d}^k\|_2^2 \leq \varepsilon^2 \tilde{M}_0. \tag{3.19}$$

On the other hand, an application of quadratic inequality, $\frac{1}{8} |\boldsymbol{d}^k|^4 - \frac{1}{2} |\boldsymbol{d}^k|^2 \geq -\frac{1}{2}$ (at a point-wise level), implies that

$$\frac{1}{8} \|\boldsymbol{d}^k\|_4^4 - \frac{1}{2} \|\boldsymbol{d}^k\|_2^2 \geq -\frac{1}{2} |\Omega|, \tag{3.20}$$

and its combination with (3.19) leads to

$$\frac{1}{8} \|\boldsymbol{d}^k\|_4^4 \leq \varepsilon^2 \tilde{M}_0 + \frac{1}{2} |\Omega|,$$

which implies that

$$\|\boldsymbol{d}^k\|_4 \leq \left(8\varepsilon^2 \tilde{M}_0 + 4|\Omega|\right)^{\frac{1}{4}} := M_0^{(4)}, \quad \forall k \geq 0. \tag{3.21}$$

We also notice that $M_0^{(4)} = O(1)$, since $\varepsilon^2 \tilde{M}_0 = O(1)$.

Moreover, a more careful substitution of (3.20) into (3.19) reveals that

$$\|\boldsymbol{d}^k\|_2^2 + \|\nabla_h \boldsymbol{d}^k\|_2^2 \leq 2(\tilde{M}_0 + \varepsilon^{-2}|\Omega|). \tag{3.22}$$

Consequently, the following estimate is available:

$$\|\boldsymbol{d}^k\|_{H_h^1} = \left(\|\boldsymbol{d}^k\|_2^2 + \|\nabla_h \boldsymbol{d}^k\|_2^2\right)^{\frac{1}{2}} \leq \sqrt{2}(\tilde{M}_0 + \varepsilon^{-2}|\Omega|)^{\frac{1}{2}} := M_0^{(1)}, \tag{3.23}$$

with $M_0^{(1)} = O(\varepsilon^{-1})$. Finally, an application of the discrete Sobolev inequality (3.13) (in Lemma 3.1) indicates that

$$\|\boldsymbol{d}^k\|_6 \leq C_1 \|\boldsymbol{d}^k\|_{H_h^1} \leq C_1 M_0^{(1)} := M_0^{(6)}, \quad \forall k \geq 0, \tag{3.24}$$

with $M_0^{(6)} = O(\varepsilon^{-1})$. This completes the proof of Corollary 3.1. □

4. Optimal rate convergence analysis

We denote $\boldsymbol{D} = \boldsymbol{d}_e$ and $P = p_e$ as the exact solutions for the phase field $\boldsymbol{d}$ and the pressure variable, respectively. For the velocity, we note that the exact velocity $\boldsymbol{u}_e$ is not divergence-free at the discrete level ($\nabla_h \cdot \boldsymbol{u}_e \neq 0$). To overcome this difficulty, we must also construct an approximate solution to the velocity vector (again through the exact solution), which satisfies the divergence-free conditions at the discrete level. In more details, for the exact velocity vector $\boldsymbol{u}_e$, there is an exact stream function vector $\boldsymbol{\psi}_e = (\psi_{1e}, \psi_{2e}, \psi_{3e})^T$ so that $\boldsymbol{u}_e = \nabla^\perp \boldsymbol{\psi}_e$. Subsequently, we construct the $\boldsymbol{U}$ as

$$\boldsymbol{U} = \nabla_h^\perp \boldsymbol{\psi}_e = (D_y \psi_{3e} - D_z \psi_{2e}, D_z \psi_{1e} - D_x \psi_{3e}, D_x \psi_{2e} - D_y \psi_{1e})^T, \tag{4.1}$$

at the staggered mesh points. In turn, we have $\nabla_h \cdot \boldsymbol{U} = 0$ at a point-wise level. In addition, we construct an approximate velocity vector $\overline{\boldsymbol{U}}$ by

$$\overline{\boldsymbol{U}}^{n+1} = \boldsymbol{U}^{n+1} + \Delta t \nabla_h (P^{n+1} - P^n), \tag{4.2}$$

at each time step. A careful Taylor expansion in time implies that

$$\|\overline{\boldsymbol{U}}^{n+1} - \boldsymbol{U}^{n+1}\|_{W_h^{2,\infty}} \leq C\Delta t^2, \quad \text{with } \|f\|_{W_h^{2,\infty}} := \|f\|_\infty + \|\nabla_h f\|_\infty + \|\nabla_h(\nabla_h f)\|_\infty. \tag{4.3}$$

Furthermore, the cell-centered grid function Γ, a numerical approximation to the chemical potential, is defined as

$$\Gamma^{n+1} := \varepsilon^{-2}((\boldsymbol{D}^{n+1})^3 - \boldsymbol{D}^n) - \Delta_h \boldsymbol{D}^{n+1}. \tag{4.4}$$

Because of the $O(\Delta t^2)$ approximation of $\overline{\boldsymbol{U}}^{n+1}$ to $\boldsymbol{U}^{n+1}$, as given by (4.2), the following local truncation error estimates for the PDE system are available:

$$\frac{\overline{\boldsymbol{U}}^{n+1} - \boldsymbol{U}^n}{\Delta t} + \frac{1}{2}(\boldsymbol{U}^n \cdot \nabla_h \overline{\boldsymbol{U}}^{n+1} + \nabla_h \cdot (\overline{\boldsymbol{U}}^{n+1}(\boldsymbol{U}^n)^T)) + \nabla_h P^n - \nu \Delta_h \overline{\boldsymbol{U}}^{n+1}$$
$$+ \lambda(\nabla_h \Gamma^{n+1})^T \boldsymbol{D}^n + \lambda \nabla_h \cdot \left(\beta \Gamma^{n+1}(\boldsymbol{D}^n)^T + (\beta+1)\boldsymbol{D}^n(\Gamma^{n+1})^T\right) = \tau_u^{n+1}, \tag{4.5}$$

$$\frac{\boldsymbol{U}^{n+1} - \overline{\boldsymbol{U}}^{n+1}}{\Delta t} + \nabla_h(P^{n+1} - P^n) = \boldsymbol{0}, \quad \nabla_h \cdot \boldsymbol{U}^{n+1} = 0, \tag{4.6}$$

$$\frac{\boldsymbol{D}^{n+1} - \boldsymbol{D}^n}{\Delta t} + \nabla_h \cdot (\boldsymbol{D}^n (\overline{\boldsymbol{U}}^{n+1})^T) + (\beta \nabla_h \overline{\boldsymbol{U}}^{n+1} + (1+\beta)(\nabla_h \overline{\boldsymbol{U}}^{n+1})^T) \boldsymbol{D}^n$$
$$= -\gamma \Gamma^{n+1} + \tau_d^{n+1}, \tag{4.7}$$

with $\|\tau_u^{n+1}\|_2, \|\tau_d^{n+1}\|_{H_h^1} \leq C(\Delta t + h^2)$.

The numerical error functions are defined as

$$\tilde{\boldsymbol{d}}^m := \boldsymbol{D}^m - \boldsymbol{d}^m, \quad \tilde{\boldsymbol{\mu}}^m := \Gamma^m - \boldsymbol{\mu}^m,$$
$$\tilde{\boldsymbol{u}}^m := \boldsymbol{U}^m - \boldsymbol{u}^m, \quad \tilde{\overline{\boldsymbol{u}}}^m := \overline{\boldsymbol{U}}^m - \overline{\boldsymbol{u}}^m, \quad \tilde{p}^m = P^m - p^m.$$

Subtracting (4.5)-(4.7) from (2.20)-(2.23) yields

$$\frac{\tilde{\overline{\boldsymbol{u}}}^{n+1} - \tilde{\boldsymbol{u}}^n}{\Delta t} + \frac{1}{2}(\boldsymbol{u}^n \cdot \nabla_h \tilde{\overline{\boldsymbol{u}}}^{n+1} + \tilde{\boldsymbol{u}}^n \cdot \nabla_h \overline{\boldsymbol{U}}^{n+1} + \nabla_h \cdot (\tilde{\overline{\boldsymbol{u}}}^{n+1}(\boldsymbol{u}^n)^T + \overline{\boldsymbol{U}}^{n+1}(\tilde{\boldsymbol{u}}^n)^T)) + \nabla_h \tilde{p}^n$$
$$- \nu \Delta_h \tilde{\overline{\boldsymbol{u}}}^{n+1} + \lambda (\nabla_h \Gamma^{n+1})^T \tilde{\boldsymbol{d}}^n + \lambda (\nabla_h \tilde{\boldsymbol{\mu}}^{n+1})^T \boldsymbol{d}^n$$
$$+ \lambda \nabla_h \cdot \left(\beta(\Gamma^{n+1}(\tilde{\boldsymbol{d}}^n)^T + \tilde{\boldsymbol{\mu}}^{n+1}(\boldsymbol{d}^n)^T) + (\beta+1)(\tilde{\boldsymbol{d}}^n(\Gamma^{n+1})^T + \boldsymbol{d}^n(\tilde{\boldsymbol{\mu}}^{n+1})^T) \right) = \tau_u^{n+1}, \tag{4.8}$$

$$\frac{\tilde{\boldsymbol{u}}^{n+1} - \tilde{\overline{\boldsymbol{u}}}^{n+1}}{\Delta t} + \nabla_h (\tilde{p}^{n+1} - \tilde{p}^n) = \boldsymbol{0}, \quad \nabla_h \cdot \tilde{\boldsymbol{u}}^{n+1} = 0, \tag{4.9}$$

$$\frac{\tilde{\boldsymbol{d}}^{n+1} - \tilde{\boldsymbol{d}}^n}{\Delta t} + \nabla_h \cdot (\tilde{\boldsymbol{d}}^n (\overline{\boldsymbol{U}}^{n+1})^T + \boldsymbol{d}^n (\tilde{\overline{\boldsymbol{u}}}^{n+1})^T) + (\beta \nabla_h \overline{\boldsymbol{U}}^{n+1} + (1+\beta)(\nabla_h \overline{\boldsymbol{U}}^{n+1})^T) \tilde{\boldsymbol{d}}^n$$
$$+ (\beta \nabla_h \tilde{\overline{\boldsymbol{u}}}^{n+1} + (1+\beta)(\nabla_h \tilde{\overline{\boldsymbol{u}}}^{n+1})^T) \boldsymbol{d}^n = -\gamma \tilde{\boldsymbol{\mu}}^{n+1} + \tau_d^{n+1}, \tag{4.10}$$

for $0 \leq n \leq M$. We also observe that $\tilde{\boldsymbol{d}}^0 \equiv 0$, $\tilde{\boldsymbol{u}}^0 \equiv 0$, and $\tilde{p}^0 = O(h^2)$.

With the assumed regularities for the exact solution, the constructed approximate solutions Γ^m and $\overline{\boldsymbol{U}}^m$ obey the following estimates:

$$\|\Gamma^m\|_\infty + \|\nabla_h \Gamma^m\|_\infty \leq C^*, \quad \|\overline{\boldsymbol{U}}^m\|_\infty + \|\nabla_h \overline{\boldsymbol{U}}^m\|_\infty \leq C^*, \quad \forall m \geq 0. \tag{4.11}$$

For the numerical solution, the uniform-in-time L_h^4 and L_h^6 bounds have been derived in (3.17) in Corollary 3.1.

Before we proceed into the detailed error estimate, we take a more careful look at the numerical error associated with the chemical potential. We begin with the following expansion:

$$\tilde{\boldsymbol{\mu}}^{n+1} = \Gamma^{n+1} - \boldsymbol{\mu}^{n+1} = \mathcal{N}_1^{n+1} - \Delta_h \tilde{\boldsymbol{d}}^{n+1}, \tag{4.12}$$

where

$$\mathcal{N}_1^{n+1} := \varepsilon^{-2} \left(|\boldsymbol{d}^{n+1}|^2 \tilde{\boldsymbol{d}}^{n+1} + ((\boldsymbol{D}^{n+1} + \boldsymbol{d}^{n+1}) \cdot \tilde{\boldsymbol{d}}^{n+1}) \boldsymbol{D}^{n+1} - \tilde{\boldsymbol{d}}^n \right). \tag{4.13}$$

Furthermore, the following preliminary results will be extensively utilized in the convergence analysis.

LEMMA 4.1. *For the nonlinear error expansion* (4.13), *we have*

$$\|\mathcal{N}_1^{n+1}\|_2 \leq \frac{3}{2} \varepsilon^{-2}((M_0^{(6)})^2 + (C^*)^2)(\|\tilde{\boldsymbol{d}}^{n+1}\|_2 + \|\nabla_h \tilde{\boldsymbol{d}}^{n+1}\|_2) + \varepsilon^{-2} \|\tilde{\boldsymbol{d}}^n\|_2, \tag{4.14}$$

$$\|\mathcal{N}_1^{n+1}\|_3 \le \frac{3}{2}\varepsilon^{-2}((M_0^{(6)})^2 + (C^*)^2)\|\tilde{\boldsymbol{d}}^{n+1}\|_\infty + \varepsilon^{-2}\|\tilde{\boldsymbol{d}}^n\|_3, \tag{4.15}$$

$$\|\nabla_h\mathcal{N}_1^{n+1}\|_{\frac{3}{2}} \le C\varepsilon^{-2}\Big(((M_0^{(6)})^2 + (M_0^{(1)})^2 + (C^*)^2)(\|\nabla_h\tilde{\boldsymbol{d}}^{n+1}\|_3 + \|\tilde{\boldsymbol{d}}^{n+1}\|_\infty) + \|\tilde{\boldsymbol{d}}^n\|_3\Big). \tag{4.16}$$

Proof.   Based on the nonlinear expansion (4.13), a careful analysis implies that

$$\|\mathcal{N}_1^{n+1}\|_2 \le \varepsilon^{-2}\Big(\|\boldsymbol{d}^{n+1}\|_6^2 \cdot \|\tilde{\boldsymbol{d}}^{n+1}\|_6 + (\|\boldsymbol{D}^{n+1}\|_6 + \|\boldsymbol{d}^{n+1}\|_6)\|\boldsymbol{D}^{n+1}\|_6 \cdot \|\tilde{\boldsymbol{d}}^{n+1}\|_6 + \|\tilde{\boldsymbol{d}}^n\|_2\Big)$$

$$\le \varepsilon^{-2}\Big(\frac{3}{2}(\|\boldsymbol{d}^{n+1}\|_6^2 + \|\boldsymbol{D}^{n+1}\|_6^2)\|\tilde{\boldsymbol{d}}^{n+1}\|_6 + \|\tilde{\boldsymbol{d}}^n\|_2\Big)$$

$$\le \frac{3}{2}\varepsilon^{-2}((M_0^{(6)})^2 + (C^*)^2)(\|\tilde{\boldsymbol{d}}^{n+1}\|_2 + \|\nabla_h\tilde{\boldsymbol{d}}^{n+1}\|_2) + \varepsilon^{-2}\|\tilde{\boldsymbol{d}}^n\|_2, \tag{4.17}$$

so that (4.14) is valid, in which the discrete Sobolev inequality (3.13) (in Lemma 3.1) has been used in the last step.

For the discrete $\|\cdot\|_3$ estimate, we apply an alternate discrete Hölder inequality and obtain

$$\|\mathcal{N}_1^{n+1}\|_3 \le \varepsilon^{-2}\Big(\|\boldsymbol{d}^{n+1}\|_6^2 \cdot \|\tilde{\boldsymbol{d}}^{n+1}\|_\infty + (\|\boldsymbol{D}^{n+1}\|_6 + \|\boldsymbol{d}^{n+1}\|_6)\|\boldsymbol{D}^{n+1}\|_6 \cdot \|\tilde{\boldsymbol{d}}^{n+1}\|_\infty + \|\tilde{\boldsymbol{d}}^n\|_3\Big)$$

$$\le \varepsilon^{-2}\Big(\frac{3}{2}(\|\boldsymbol{d}^{n+1}\|_6^2 + \|\boldsymbol{D}^{n+1}\|_6^2)\|\tilde{\boldsymbol{d}}^{n+1}\|_\infty + \|\tilde{\boldsymbol{d}}^n\|_3\Big)$$

$$\le \frac{3}{2}\varepsilon^{-2}((M_0^{(6)})^2 + (C^*)^2)\|\tilde{\boldsymbol{d}}^{n+1}\|_\infty + \varepsilon^{-2}\|\tilde{\boldsymbol{d}}^n\|_3, \tag{4.18}$$

so that (4.15) has been proved.

Similarly, for the gradient of $\mathcal{N}_1^{n+1}$, we carry out a local expansion and get the following estimate:

$$\|\nabla_h\mathcal{N}_1^{n+1}\|_{\frac{3}{2}} \le C\varepsilon^{-2}\Big(\|\boldsymbol{d}^{n+1}\|_6^2 \cdot \|\nabla_h\tilde{\boldsymbol{d}}^{n+1}\|_3 + \|\boldsymbol{d}^{n+1}\|_6 \cdot \|\nabla_h\boldsymbol{d}^{n+1}\|_2 \cdot \|\tilde{\boldsymbol{d}}^{n+1}\|_\infty$$

$$+ (\|\boldsymbol{D}^{n+1}\|_6 + \|\boldsymbol{d}^{n+1}\|_6)\|\boldsymbol{D}^{n+1}\|_6 \cdot \|\nabla_h\tilde{\boldsymbol{d}}^{n+1}\|_3$$

$$+ (\|\boldsymbol{D}^{n+1}\|_6 + \|\boldsymbol{d}^{n+1}\|_6)(\|\nabla_h\boldsymbol{D}^{n+1}\|_2 + \|\nabla_h\boldsymbol{d}^{n+1}\|_2) \cdot \|\tilde{\boldsymbol{d}}^{n+1}\|_\infty + \|\tilde{\boldsymbol{d}}^n\|_{\frac{3}{2}}\Big)$$

$$\le C\varepsilon^{-2}\Big((\|\boldsymbol{d}^{n+1}\|_6^2 + \|\boldsymbol{D}^{n+1}\|_6^2)(\|\nabla_h\tilde{\boldsymbol{d}}^{n+1}\|_3 + \|\tilde{\boldsymbol{d}}^{n+1}\|_\infty) + \|\tilde{\boldsymbol{d}}^n\|_3\Big)$$

$$\le C\varepsilon^{-2}\Big(((M_0^{(6)})^2 + (M_0^{(1)})^2 + (C^*)^2)(\|\nabla_h\tilde{\boldsymbol{d}}^{n+1}\|_3 + \|\tilde{\boldsymbol{d}}^{n+1}\|_\infty) + \|\tilde{\boldsymbol{d}}^n\|_3\Big), \tag{4.19}$$

so that (4.16) becomes available. This finishes the proof of Lemma 4.1.   □

4.1.   The $L_{\Delta t}^\infty(0,T;L_h^2) \cap L_{\Delta t}^2(0,T;H_h^1)$ error estimate for the phase field equation.   Taking a discrete inner product with (4.10) by $\tilde{\boldsymbol{d}}^{n+1}$ gives

$$\Delta t\langle\tau_d^{n+1}, \tilde{\boldsymbol{d}}^{n+1}\rangle_C = \frac{1}{2}(\|\tilde{\boldsymbol{d}}^{n+1}\|_2^2 - \|\tilde{\boldsymbol{d}}^n\|_2^2 + \|\tilde{\boldsymbol{d}}^{n+1} - \tilde{\boldsymbol{d}}^n\|_2^2) + \gamma\Delta t\langle\tilde{\boldsymbol{\mu}}^{n+1}, \tilde{\boldsymbol{d}}^{n+1}\rangle_C$$

$$- \Delta t\langle\tilde{\boldsymbol{d}}^n(\overline{\boldsymbol{U}}^{n+1})^T + \boldsymbol{d}^n(\tilde{\overline{\boldsymbol{u}}}^{n+1})^T, \nabla_h\tilde{\boldsymbol{d}}^{n+1}\rangle_1$$

$$+ \Delta t\langle(\beta\nabla_h\overline{\boldsymbol{U}}^{n+1} + (1+\beta)(\nabla_h\overline{\boldsymbol{U}}^{n+1})^T)\tilde{\boldsymbol{d}}^n, \tilde{\boldsymbol{d}}^{n+1}\rangle_C$$

$$+ \Delta t\langle(\beta\nabla_h\tilde{\overline{\boldsymbol{u}}}^{n+1} + (1+\beta)(\nabla_h\tilde{\overline{\boldsymbol{u}}}^{n+1})^T)\boldsymbol{d}^n, \tilde{\boldsymbol{d}}^{n+1}\rangle_C. \tag{4.20}$$

The bound for the local truncation error term is straightforward:

$$\langle \tau_d^{n+1}, \tilde{\boldsymbol{d}}^{n+1}\rangle_C \leq \frac{1}{2}(\|\tau_d^{n+1}\|_2^2 + \|\tilde{\boldsymbol{d}}^{n+1}\|_2^2). \tag{4.21}$$

For the term associated with the chemical potential dissipation, we make use of the expansion (4.12), and arrive at

$$\langle \tilde{\boldsymbol{\mu}}^{n+1}, \tilde{\boldsymbol{d}}^{n+1}\rangle_C \geq -\varepsilon^{-2}\langle \tilde{\boldsymbol{d}}^n, \tilde{\boldsymbol{d}}^{n+1}\rangle_C + \|\nabla_h \tilde{\boldsymbol{d}}^{n+1}\|_2^2$$
$$\geq -\frac{\varepsilon^{-2}}{2}(\|\tilde{\boldsymbol{d}}^n\|_2^2 + \|\tilde{\boldsymbol{d}}^{n+1}\|_2^2) + \|\nabla_h \tilde{\boldsymbol{d}}^{n+1}\|_2^2. \tag{4.22}$$

For the nonlinear terms, the following parts could be analyzed based on the regularity estimates (4.11):

$$\langle \tilde{\boldsymbol{d}}^n(\overline{\boldsymbol{U}}^{n+1})^T, \nabla_h \tilde{\boldsymbol{d}}^{n+1}\rangle_1 \leq C^*\|\tilde{\boldsymbol{d}}^n\|_2 \cdot \|\nabla_h \tilde{\boldsymbol{d}}^{n+1}\|_2$$
$$\leq 2(C^*)^2\gamma^{-1}\|\tilde{\boldsymbol{d}}^n\|_2^2 + \frac{\gamma}{8}\|\nabla_h \tilde{\boldsymbol{d}}^{n+1}\|_2^2, \tag{4.23}$$

$$-\beta\langle \nabla_h \overline{\boldsymbol{U}}^{n+1}\tilde{\boldsymbol{d}}^n, \tilde{\boldsymbol{d}}^{n+1}\rangle_C \leq \beta C^*\|\tilde{\boldsymbol{d}}^n\|_2 \cdot \|\tilde{\boldsymbol{d}}^{n+1}\|_2 \leq \frac{\beta C^*}{2}(\|\tilde{\boldsymbol{d}}^n\|_2^2 + \|\tilde{\boldsymbol{d}}^{n+1}\|_2^2), \tag{4.24}$$

$$-(1+\beta)\langle (\nabla_h \overline{\boldsymbol{U}}^{n+1})^T\tilde{\boldsymbol{d}}^n, \tilde{\boldsymbol{d}}^{n+1}\rangle_C \leq (1+\beta)C^*\|\tilde{\boldsymbol{d}}^n\|_2 \cdot \|\tilde{\boldsymbol{d}}^{n+1}\|_2$$
$$\leq \frac{(1+\beta)C^*}{2}(\|\tilde{\boldsymbol{d}}^n\|_2^2 + \|\tilde{\boldsymbol{d}}^{n+1}\|_2^2). \tag{4.25}$$

For the nonlinear term $\langle \boldsymbol{d}^n\tilde{\tilde{\boldsymbol{u}}}^{n+1}, \nabla_h \tilde{\boldsymbol{d}}^{n+1}\rangle_1$, the following analysis could be performed:

$$\langle \boldsymbol{d}^n(\tilde{\tilde{\boldsymbol{u}}}^{n+1})^T, \nabla_h \tilde{\boldsymbol{d}}^{n+1}\rangle_1 \leq \|\boldsymbol{d}^n\|_4 \cdot \|\tilde{\tilde{\boldsymbol{u}}}^{n+1}\|_4 \cdot \|\nabla_h \tilde{\boldsymbol{d}}^{n+1}\|_2 \leq M_0^{(4)}\|\tilde{\tilde{\boldsymbol{u}}}^{n+1}\|_4 \cdot \|\nabla_h \tilde{\boldsymbol{d}}^{n+1}\|_2$$
$$\leq 4(M_0^{(4)})^2\gamma^{-1}\|\tilde{\tilde{\boldsymbol{u}}}^{n+1}\|_4^2 + \frac{\gamma}{8}\|\nabla_h \tilde{\boldsymbol{d}}^{n+1}\|_4^2. \tag{4.26}$$

The two other nonlinear terms could be analyzed in a similar manner:

$$-\beta\langle \nabla_h \tilde{\tilde{\boldsymbol{u}}}^{n+1}\boldsymbol{d}^n, \tilde{\boldsymbol{d}}^{n+1}\rangle_C$$
$$\leq \beta\|\nabla_h \tilde{\tilde{\boldsymbol{u}}}^{n+1}\|_2 \cdot \|\boldsymbol{d}^n\|_4 \cdot \|\tilde{\boldsymbol{d}}^{n+1}\|_4 \leq \beta M_0^{(4)}\|\nabla_h \tilde{\tilde{\boldsymbol{u}}}^{n+1}\|_2 \cdot \|\tilde{\boldsymbol{d}}^{n+1}\|_4$$
$$\leq \frac{\nu}{8\lambda}\|\nabla_h \tilde{\tilde{\boldsymbol{u}}}^{n+1}\|_2^2 + 2\beta^2(M_0^{(4)})^2\lambda\nu^{-1}\|\tilde{\boldsymbol{d}}^{n+1}\|_4^2, \tag{4.27}$$

$$-(1+\beta)\langle (\nabla_h \tilde{\tilde{\boldsymbol{u}}}^{n+1})^T\boldsymbol{d}^n, \tilde{\boldsymbol{d}}^{n+1}\rangle_C \leq (1+\beta)\|\nabla_h \tilde{\tilde{\boldsymbol{u}}}^{n+1}\|_2 \cdot \|\boldsymbol{d}^n\|_4 \cdot \|\tilde{\boldsymbol{d}}^{n+1}\|_4$$
$$\leq (1+\beta)M_0^{(4)}\|\nabla_h \tilde{\tilde{\boldsymbol{u}}}^{n+1}\|_2 \cdot \|\tilde{\boldsymbol{d}}^{n+1}\|_4$$
$$\leq \frac{\nu}{8\lambda}\|\nabla_h \tilde{\tilde{\boldsymbol{u}}}^{n+1}\|_2^2 + 2(1+\beta)^2(M_0^{(4)})^2\lambda\nu^{-1}\|\tilde{\boldsymbol{d}}^{n+1}\|_4^2. \tag{4.28}$$

Subsequently, a substitution of (4.21), (4.22), (4.23)-(4.25), (4.26)-(4.28) into (4.20) results in

$$\|\tilde{\boldsymbol{d}}^{n+1}\|_2^2 - \|\tilde{\boldsymbol{d}}^n\|_2^2 + \frac{5}{4}\gamma\Delta t\|\nabla_h \tilde{\boldsymbol{d}}^{n+1}\|_2^2 - \frac{\nu}{2}\Delta t\|\nabla_h \tilde{\tilde{\boldsymbol{u}}}^{n+1}\|_2^2$$
$$\leq D_{11}^n\Delta t(\|\tilde{\boldsymbol{d}}^n\|_2^2 + \|\tilde{\boldsymbol{d}}^{n+1}\|_2^2) + D_2^{n+1}\Delta t\|\tilde{\tilde{\boldsymbol{u}}}^{n+1}\|_4^2 + D_3^{n+1}\Delta t\|\tilde{\boldsymbol{d}}^{n+1}\|_4^2 + \Delta t\|\tau_d^{n+1}\|_2^2, \tag{4.29}$$

where

$$
\begin{aligned}
D_{11}^n &:= \varepsilon^{-2} + 4(C^*)^2 \gamma^{-1} + (2\beta+1)C^* + 1, \\
D_2^{n+1} &:= 8(M_0^{(4)})^2 \gamma^{-1}, \\
D_3^{n+1} &:= 4(2\beta^2 + 2\beta + 1)(M_0^{(4)})^2 \lambda \nu^{-1}.
\end{aligned}
\tag{4.30}
$$

4.2. The $L_{\Delta t}^\infty(0,T;L_h^2) \cap L_{\Delta t}^2(0,T;H_h^1)$ error estimate for the momentum equation. Taking a discrete inner product of (4.8) with $\tilde{\tilde{\boldsymbol{u}}}^{n+1}$ gives

$$
\frac{1}{2\Delta t}(\|\tilde{\tilde{\boldsymbol{u}}}^{n+1}\|_2^2 - \|\tilde{\boldsymbol{u}}^n\|_2^2 + \|\tilde{\tilde{\boldsymbol{u}}}^{n+1} - \tilde{\boldsymbol{u}}^n\|_2^2) + \nu\|\nabla_h \tilde{\tilde{\boldsymbol{u}}}^{n+1}\|_2^2 + \langle \nabla_h \tilde{p}^n, \tilde{\tilde{\boldsymbol{u}}}^{n+1}\rangle_1 - \langle \tau_u^{n+1}, \tilde{\tilde{\boldsymbol{u}}}^{n+1}\rangle_1
$$
$$
+ \frac{1}{2}\langle \boldsymbol{u}^n \cdot \nabla_h \tilde{\tilde{\boldsymbol{u}}}^{n+1} + \tilde{\boldsymbol{u}}^n \cdot \nabla_h \overline{\boldsymbol{U}}^{n+1} + \nabla_h \cdot (\tilde{\tilde{\boldsymbol{u}}}^{n+1}(\boldsymbol{u}^n)^T + \overline{\boldsymbol{U}}^{n+1}(\tilde{\boldsymbol{u}}^n)^T), \tilde{\tilde{\boldsymbol{u}}}^{n+1}\rangle_1
$$
$$
+ \lambda\langle (\nabla_h \Gamma^{n+1})^T \tilde{\boldsymbol{d}}^n, \tilde{\tilde{\boldsymbol{u}}}^{n+1}\rangle_1 + \lambda\langle \Gamma^{n+1}, \left(\beta(\nabla_h \tilde{\tilde{\boldsymbol{u}}}^{n+1}) + (\beta+1)(\nabla_h \tilde{\tilde{\boldsymbol{u}}}^{n+1})^T\right)\tilde{\boldsymbol{d}}^n\rangle_C
$$
$$
+ \lambda\langle (\nabla_h \tilde{\boldsymbol{\mu}}^{n+1})^T \boldsymbol{d}^n, \tilde{\tilde{\boldsymbol{u}}}^{n+1}\rangle_1 + \lambda\langle \tilde{\boldsymbol{\mu}}^{n+1}, \left(\beta(\nabla_h \tilde{\tilde{\boldsymbol{u}}}^{n+1}) + (\beta+1)(\nabla_h \tilde{\tilde{\boldsymbol{u}}}^{n+1})^T\right)\boldsymbol{d}^n\rangle_C = 0, \tag{4.31}
$$

in which the summation by parts formulas (2.34)-(2.39) have been repeatedly applied. Similarly, the bound for the local truncation error term is standard:

$$
\langle \tau_u^{n+1}, \tilde{\tilde{\boldsymbol{u}}}^{n+1}\rangle_1 \le \frac{1}{2}(\|\tau_u^{n+1}\|_2^2 + \|\tilde{\tilde{\boldsymbol{u}}}^{n+1}\|_2^2). \tag{4.32}
$$

For the pressure gradient term, the following analysis could be performed:

$$
\begin{aligned}
\langle \nabla_h \tilde{p}^n, \tilde{\tilde{\boldsymbol{u}}}^{n+1}\rangle_1 &= -\langle \tilde{p}^n, \nabla_h \cdot \tilde{\tilde{\boldsymbol{u}}}^{n+1}\rangle_C \\
&= -\langle \tilde{p}^n, \Delta t \Delta_h(\tilde{p}^{n+1} - \tilde{p}^n)\rangle_C = \Delta t\langle \nabla_h \tilde{p}^n, \nabla_h(\tilde{p}^{n+1} - \tilde{p}^n)\rangle_1 \\
&= \frac{\Delta t}{2}(\|\nabla_h \tilde{p}^{n+1}\|_2^2 - \|\nabla_h \tilde{p}^n\|_2^2) - \frac{\Delta t}{2}\|\nabla_h(\tilde{p}^{n+1} - \tilde{p}^n)\|_2^2 \\
&= \frac{\Delta t}{2}(\|\nabla_h \tilde{p}^{n+1}\|_2^2 - \|\nabla_h \tilde{p}^n\|_2^2) - \frac{1}{2\Delta t}\|\tilde{\boldsymbol{u}}^{n+1} - \tilde{\tilde{\boldsymbol{u}}}^{n+1}\|_2^2, \tag{4.33}
\end{aligned}
$$

in which the numerical error Equation (4.8) has been repeatedly applied in the derivation. For the linearized fluid convection terms, we make the following observation;

$$
\langle \boldsymbol{u}^n \cdot \nabla_h \tilde{\tilde{\boldsymbol{u}}}^{n+1} + \nabla_h \cdot (\tilde{\tilde{\boldsymbol{u}}}^{n+1}(\boldsymbol{u}^n)^T), \tilde{\tilde{\boldsymbol{u}}}^{n+1}\rangle_1 = 0, \tag{4.34}
$$

which comes from the summation by parts formula. The remaining two terms in the fluid convection part could be controlled in a standard way:

$$
-\langle \tilde{\boldsymbol{u}}^n \cdot \nabla_h \overline{\boldsymbol{U}}^{n+1}, \tilde{\tilde{\boldsymbol{u}}}^{n+1}\rangle_1 \le C^*\|\tilde{\boldsymbol{u}}^n\|_2 \cdot \|\tilde{\tilde{\boldsymbol{u}}}^{n+1}\|_2 \le \frac{C^*}{2}(\|\tilde{\boldsymbol{u}}^n\|_2^2 + \|\tilde{\tilde{\boldsymbol{u}}}^{n+1}\|_2^2), \tag{4.35}
$$

$$
\begin{aligned}
-\langle \nabla_h \cdot (\overline{\boldsymbol{U}}^{n+1}(\tilde{\boldsymbol{u}}^n)^T), \tilde{\tilde{\boldsymbol{u}}}^{n+1}\rangle_1 &= \langle \overline{\boldsymbol{U}}^{n+1}(\tilde{\boldsymbol{u}}^n)^T, \nabla_h \tilde{\tilde{\boldsymbol{u}}}^{n+1}\rangle \le C^*\|\tilde{\boldsymbol{u}}^n\|_2 \cdot \|\nabla_h \tilde{\tilde{\boldsymbol{u}}}^{n+1}\|_2 \\
&\le 2(C^*)^2\nu^{-1}\|\tilde{\boldsymbol{u}}^n\|_2^2 + \frac{\nu}{8}\|\nabla_h \tilde{\tilde{\boldsymbol{u}}}^{n+1}\|_2, \tag{4.36}
\end{aligned}
$$

with an application of the regularity estimates (4.11).

The next three nonlinear inner product terms could be controlled via a similar approach:

$$
-\lambda\langle (\nabla_h \Gamma^{n+1})^T \tilde{\boldsymbol{d}}^n, \tilde{\tilde{\boldsymbol{u}}}^{n+1}\rangle_1 \le C^*\lambda\|\tilde{\boldsymbol{d}}^n\|_2 \cdot \|\tilde{\tilde{\boldsymbol{u}}}^{n+1}\|_2 \le \frac{C^*\lambda}{2}(\|\tilde{\boldsymbol{d}}^n\|_2^2 + \|\tilde{\tilde{\boldsymbol{u}}}^{n+1}\|_2^2), \tag{4.37}
$$

$$\beta\lambda\langle\Gamma^{n+1},(\nabla_h\tilde{\tilde{\boldsymbol{u}}}^{n+1})\tilde{\boldsymbol{d}}^n\rangle_C \le \beta C^*\lambda\|\tilde{\boldsymbol{d}}^n\|_2\cdot\|\nabla_h\tilde{\tilde{\boldsymbol{u}}}^{n+1}\|_2$$
$$\le 4(\beta C^*\lambda)^2\nu^{-1}\|\tilde{\boldsymbol{d}}^n\|_2^2+\frac{\nu}{16}\|\nabla_h\tilde{\tilde{\boldsymbol{u}}}^{n+1}\|_2^2, \tag{4.38}$$

$$(1+\beta)\lambda\langle\Gamma^{n+1},(\nabla_h\tilde{\tilde{\boldsymbol{u}}}^{n+1})^T\tilde{\boldsymbol{d}}^n\rangle_C \le (1+\beta)C^*\lambda\|\tilde{\boldsymbol{d}}^n\|_2\cdot\|\nabla_h\tilde{\tilde{\boldsymbol{u}}}^{n+1}\|_2$$
$$\le 4((1+\beta)C^*\lambda)^2\nu^{-1}\|\tilde{\boldsymbol{d}}^n\|_2^2+\frac{\nu}{16}\|\nabla_h\tilde{\tilde{\boldsymbol{u}}}^{n+1}\|_2^2. \tag{4.39}$$

For the remaining three nonlinear inner product terms, we have to make use of the chemical potential error expansion (4.12) and apply the corresponding estimates in Lemma 4.1. In more details, we begin with the following identity

$$-\lambda\langle(\nabla_h\tilde{\boldsymbol{\mu}}^{n+1})^T\boldsymbol{d}^n,\tilde{\tilde{\boldsymbol{u}}}^{n+1}\rangle_1$$
$$=\lambda\langle(\nabla_h\Delta_h\boldsymbol{d}^{n+1})^T\boldsymbol{d}^n,\tilde{\tilde{\boldsymbol{u}}}^{n+1}\rangle_1-\lambda\langle(\nabla_h\mathcal{N}_1^{n+1})^T\boldsymbol{d}^n,\tilde{\tilde{\boldsymbol{u}}}^{n+1}\rangle_1. \tag{4.40}$$

For the second term on the right-hand side, the following analysis is undertaken:

$$-\lambda\langle(\nabla_h\mathcal{N}_1^{n+1})^T\boldsymbol{d}^n,\tilde{\tilde{\boldsymbol{u}}}^{n+1}\rangle_1$$
$$\le \lambda\|\nabla_h\mathcal{N}_1^{n+1}\|_{\frac{3}{2}}\cdot\|\boldsymbol{d}^n\|_6\cdot\|\tilde{\tilde{\boldsymbol{u}}}^{n+1}\|_6$$
$$\le C_1\lambda M_0^{(6)}(\|\tilde{\tilde{\boldsymbol{u}}}^{n+1}\|_2+\|\nabla_h\tilde{\tilde{\boldsymbol{u}}}^{n+1}\|_2)\|\nabla_h\mathcal{N}_1^{n+1}\|_{\frac{3}{2}}$$
$$\le \frac{C_1\lambda M_0^{(6)}}{2}\|\tilde{\tilde{\boldsymbol{u}}}^{n+1}\|_2^2+\frac{\nu}{16}\|\nabla_h\tilde{\tilde{\boldsymbol{u}}}^{n+1}\|_2^2+C_5\|\nabla_h\mathcal{N}_1^{n+1}\|_{\frac{3}{2}}^2, \tag{4.41}$$

with $C_5=\frac{C_1\lambda M_0^{(6)}}{2}+4(C_1\lambda M_0^{(6)})^2\nu^{-1}$. Moreover, with an application of (4.16) in Lemma 4.1, we obtain

$$-\lambda\langle(\nabla_h\tilde{\boldsymbol{\mu}}^{n+1})^T\boldsymbol{d}^n,\tilde{\tilde{\boldsymbol{u}}}^{n+1}\rangle_1$$
$$\le\lambda\langle(\nabla_h\Delta_h\boldsymbol{d}^{n+1})^T\boldsymbol{d}^n,\tilde{\tilde{\boldsymbol{u}}}^{n+1}\rangle_1+\frac{C_1\lambda M_0^{(6)}}{2}\|\tilde{\tilde{\boldsymbol{u}}}^{n+1}\|_2^2+\frac{\nu}{16}\|\nabla_h\tilde{\tilde{\boldsymbol{u}}}^{n+1}\|_2^2$$
$$+C_6\varepsilon^{-4}(\|\nabla_h\tilde{\boldsymbol{d}}^{n+1}\|_3^2+\|\tilde{\boldsymbol{d}}^{n+1}\|_\infty^2+\|\tilde{\boldsymbol{d}}^n\|_3^2), \tag{4.42}$$

with $C_6=CC_5((M_0^{(6)})^4+(M_0^{(1)})^4+(C^*)^4+1)$. Similarly, the last two nonlinear inner product terms could be analyzed as follows:

$$\beta\lambda\langle\mathcal{N}_1^{n+1},(\nabla_h\tilde{\tilde{\boldsymbol{u}}}^{n+1})\boldsymbol{d}^n\rangle_C$$
$$\le\beta\lambda\|\mathcal{N}_1^{n+1}\|_3\cdot\|\boldsymbol{d}^n\|_6\cdot\|\nabla_h\tilde{\tilde{\boldsymbol{u}}}^{n+1}\|_2$$
$$\le\beta\lambda M_0^{(6)}\|\mathcal{N}_1^{n+1}\|_3\cdot\|\nabla_h\tilde{\tilde{\boldsymbol{u}}}^{n+1}\|_2$$
$$\le 2(\beta\lambda M_0^{(6)})^2\nu^{-1}\|\mathcal{N}_1^{n+1}\|_3^2+\frac{\nu}{8}\|\nabla_h\tilde{\tilde{\boldsymbol{u}}}^{n+1}\|_2^2, \tag{4.43}$$

$$\beta\lambda\langle\tilde{\boldsymbol{\mu}}^{n+1},(\nabla_h\tilde{\tilde{\boldsymbol{u}}}^{n+1})\boldsymbol{d}^n\rangle_C$$
$$=-\beta\lambda\langle\Delta_h\tilde{\boldsymbol{d}}^{n+1},(\nabla_h\tilde{\tilde{\boldsymbol{u}}}^{n+1})\boldsymbol{d}^n\rangle_C+\beta\lambda\langle\mathcal{N}_1^{n+1},(\nabla_h\tilde{\tilde{\boldsymbol{u}}}^{n+1})\boldsymbol{d}^n\rangle_C$$
$$\le-\beta\lambda\langle(\nabla_h\tilde{\tilde{\boldsymbol{u}}}^{n+1})\boldsymbol{d}^n,\Delta_h\tilde{\boldsymbol{d}}^{n+1}\rangle+\frac{\nu}{8}\|\nabla_h\tilde{\tilde{\boldsymbol{u}}}^{n+1}\|_2^2+2(\beta\lambda M_0^{(6)})^2\nu^{-1}\|\mathcal{N}_1^{n+1}\|_3^2$$
$$\le-\beta\lambda\langle(\nabla_h\tilde{\tilde{\boldsymbol{u}}}^{n+1})\boldsymbol{d}^n,\Delta_h\tilde{\boldsymbol{d}}^{n+1}\rangle+\frac{\nu}{8}\|\nabla_h\tilde{\tilde{\boldsymbol{u}}}^{n+1}\|_2^2+\varepsilon^{-4}(C_7\|\tilde{\boldsymbol{d}}^{n+1}\|_\infty^2+C_8\|\tilde{\boldsymbol{d}}^n\|_3^2), \tag{4.44}$$

with $C_7=36(\beta\lambda M_0^{(6)})^2\nu^{-1}((M_0^{(6)})^4+(C^*)^4)$, $C_8=4(\beta\lambda M_0^{(6)})^2\nu^{-1}$,

$$(1+\beta)\lambda\langle\mathcal{N}_1^{n+1},(\nabla_h\tilde{\tilde{\boldsymbol{u}}}^{n+1})^T\boldsymbol{d}^n\rangle_C \le (1+\beta)\lambda\|\mathcal{N}_1^{n+1}\|_3\cdot\|\boldsymbol{d}^n\|_6\cdot\|\nabla_h\tilde{\tilde{\boldsymbol{u}}}^{n+1}\|_2$$

$$\leq (1+\beta)\lambda M_0^{(6)}\|\mathcal{N}_1^{n+1}\|_3 \cdot \|\nabla_h \tilde{\tilde{\boldsymbol{u}}}^{n+1}\|_2$$
$$\leq 2((1+\beta)\lambda M_0^{(6)})^2\nu^{-1}\|\mathcal{N}_1^{n+1}\|_3^2 + \frac{\nu}{8}\|\nabla_h \tilde{\tilde{\boldsymbol{u}}}^{n+1}\|_2^2, \quad (4.45)$$

$$(1+\beta)\lambda\langle \tilde{\boldsymbol{\mu}}^{n+1}, (\nabla_h \tilde{\tilde{\boldsymbol{u}}}^{n+1})^T \boldsymbol{d}^n\rangle_C$$
$$= -(1+\beta)\lambda\langle \Delta_h \tilde{\boldsymbol{d}}^{n+1}, (\nabla_h \tilde{\tilde{\boldsymbol{u}}}^{n+1})^T \boldsymbol{d}^n\rangle_C + (1+\beta)\lambda\langle \mathcal{N}_1^{n+1}, (\nabla_h \tilde{\tilde{\boldsymbol{u}}}^{n+1})^T \boldsymbol{d}^n\rangle_C$$
$$\leq -(1+\beta)\lambda\langle (\nabla_h \tilde{\tilde{\boldsymbol{u}}}^{n+1})^T \boldsymbol{d}^n, \Delta_h \tilde{\boldsymbol{d}}^{n+1}\rangle_C + \frac{\nu}{8}\|\nabla_h \tilde{\tilde{\boldsymbol{u}}}^{n+1}\|_2^2 + 2((1+\beta)\lambda M_0^{(6)})^2\nu^{-1}\|\mathcal{N}_1^{n+1}\|_3^2$$
$$\leq -(1+\beta)\lambda\langle (\nabla_h \tilde{\tilde{\boldsymbol{u}}}^{n+1})^T \boldsymbol{d}^n, \Delta_h \tilde{\boldsymbol{d}}^{n+1}\rangle_C + \frac{\nu}{8}\|\nabla_h \tilde{\tilde{\boldsymbol{u}}}^{n+1}\|_2^2 + \varepsilon^{-4}(C_9\|\tilde{\boldsymbol{d}}^{n+1}\|_\infty^2 + C_{10}\|\tilde{\boldsymbol{d}}^n\|_3^2),$$
$$(4.46)$$

with $C_9 = 36((1+\beta)\lambda M_0^{(6)})^2\nu^{-1}((M_0^{(6)})^4 + (C^*)^4)$, $C_{10} = 4((1+\beta)\lambda M_0^{(6)})^2\nu^{-1}$.

Meanwhile, for the other velocity error Equation (4.9), its discrete inner product with $\tilde{\boldsymbol{u}}^{n+1}$ implies that

$$\|\tilde{\boldsymbol{u}}^{n+1}\|_2^2 - \|\tilde{\tilde{\boldsymbol{u}}}^{n+1}\|_2^2 + \|\tilde{\boldsymbol{u}}^{n+1} - \tilde{\tilde{\boldsymbol{u}}}^{n+1}\|_2^2 = 0, \quad \text{since } \langle \tilde{\boldsymbol{u}}^{n+1}, \nabla_h(\tilde{p}^{n+1} - \tilde{p}^n)\rangle_1 = 0. \quad (4.47)$$

Subsequently, we substitute (4.32), (4.33), (4.34)-(4.36), (4.37)-(4.39), (4.42), (4.44), (4.46) into (4.31), in combination with (4.47), and obtain

$$\|\tilde{\boldsymbol{u}}^{n+1}\|_2^2 - \|\tilde{\boldsymbol{u}}^n\|_2^2 + \|\tilde{\tilde{\boldsymbol{u}}}^{n+1} - \boldsymbol{u}^n\|_2^2 + \Delta t^2(\|\nabla_h \tilde{p}^{n+1}\|_2^2 - \|\nabla_h \tilde{p}^n\|_2^2) + \nu\Delta t\|\nabla_h \tilde{\tilde{\boldsymbol{u}}}^{n+1}\|_2^2$$
$$\leq 2\lambda\Delta t\langle (\nabla_h \Delta_h \tilde{\boldsymbol{d}}^{n+1})^T \boldsymbol{d}^n, \tilde{\boldsymbol{u}}^{n+1}\rangle_1 - 2\lambda\Delta t\langle (\beta\nabla_h \tilde{\tilde{\boldsymbol{u}}}^{n+1} + (1+\beta)(\nabla_h \tilde{\tilde{\boldsymbol{u}}}^{n+1})^T)\boldsymbol{d}^n, \Delta_h \tilde{\boldsymbol{d}}^{n+1}\rangle_C$$
$$+ D_{12}^n\Delta t\|\tilde{\boldsymbol{d}}^n\|_2^2 + D_4^n\Delta t\|\tilde{\boldsymbol{u}}^n\|_2^2 + D_5^{n+1}\Delta t\|\tilde{\tilde{\boldsymbol{u}}}^{n+1}\|_2^2 + \Delta t\|\tau_u^{n+1}\|_2^2$$
$$+ 2\varepsilon^{-4}\Delta t(C_6\|\nabla_h \tilde{\boldsymbol{d}}^{n+1}\|_3^2 + (C_6 + C_7 + C_9)\|\tilde{\boldsymbol{d}}^{n+1}\|_\infty^2 + (C_6 + C_8 + C_{10})\|\tilde{\boldsymbol{d}}^n\|_3^2), \quad (4.48)$$

with $D_{12}^n = C^*\lambda + 8(2\beta^2 + 2\beta + 1)(C^*\lambda)^2\nu^{-1}$, $\quad D_4^n = \dfrac{C^*}{2} + 2(C^*)^2\nu^{-1}$,

$$D_5^{n+1} = C^*(\frac{1}{2} + \lambda) + C_1\lambda M_0^{(6)} + 1. \quad (4.49)$$

4.3. The $L_{\Delta t}^\infty(0,T;H_h^1)\cap L_{\Delta t}^2(0,T;H_h^2)$ error estimate for the phase field equation. Taking a discrete inner product with (4.10) by $-\Delta_h \tilde{\boldsymbol{d}}^{n+1}$ gives

$$\frac{1}{2}(\|\nabla_h \tilde{\boldsymbol{d}}^{n+1}\|_2^2 - \|\nabla_h \tilde{\boldsymbol{d}}^n\|_2^2 + \|\nabla_h(\tilde{\boldsymbol{d}}^{n+1} - \tilde{\boldsymbol{d}}^n)\|_2^2) - \gamma\Delta t\langle \tilde{\boldsymbol{\mu}}^{n+1}, \Delta_h \tilde{\boldsymbol{d}}^{n+1}\rangle_C$$
$$- \Delta t\langle \nabla_h \cdot (\tilde{\boldsymbol{d}}^n(\overline{\boldsymbol{U}}^{n+1})^T), \Delta_h \tilde{\boldsymbol{d}}^{n+1}\rangle_C + \Delta t\langle \tilde{\tilde{\boldsymbol{u}}}^{n+1}, (\nabla_h \Delta_h \tilde{\boldsymbol{d}}^{n+1})^T \boldsymbol{d}^n\rangle_1$$
$$- \Delta t\langle (\beta\nabla_h \overline{\boldsymbol{U}}^{n+1} + (1+\beta)(\nabla_h \overline{\boldsymbol{U}}^{n+1})^T)\tilde{\boldsymbol{d}}^n, \Delta_h \tilde{\boldsymbol{d}}^{n+1}\rangle_C$$
$$- \Delta t\langle (\beta\nabla_h \tilde{\tilde{\boldsymbol{u}}}^{n+1} + (1+\beta)(\nabla_h \tilde{\tilde{\boldsymbol{u}}}^{n+1})^T)\boldsymbol{d}^n, \Delta_h \tilde{\boldsymbol{d}}^{n+1}\rangle_C = -\Delta t\langle \tau_d^{n+1}, \Delta_h \tilde{\boldsymbol{d}}^{n+1}\rangle_C. \quad (4.50)$$

The term associated with the local truncation error could be bounded as follows:

$$-\langle \tau_d^{n+1}, \Delta_h \tilde{\boldsymbol{d}}^{n+1}\rangle_C = \langle \nabla_h \tau_d^{n+1}, \nabla_h \tilde{\boldsymbol{d}}^{n+1}\rangle_1 \leq \frac{1}{2}(\|\nabla_h \tau_d^{n+1}\|_2^2 + \|\nabla_h \tilde{\boldsymbol{d}}^{n+1}\|_2^2). \quad (4.51)$$

For the term associated with the chemical potential dissipation, we recall the expansion (4.12), as well as the estimate (4.14) (in Lemma 4.1), and arrive at the following inequality:

$$-\langle \tilde{\boldsymbol{\mu}}^{n+1}, \Delta_h \tilde{\boldsymbol{d}}^{n+1}\rangle_C$$

$$\begin{aligned}
&= \|\Delta_h \tilde{\boldsymbol{d}}^{n+1}\|_2^2 - \langle \mathcal{N}_1^{n+1}, \Delta_h \tilde{\boldsymbol{d}}^{n+1} \rangle_C \\
&\geq \|\Delta_h \tilde{\boldsymbol{d}}^{n+1}\|_2^2 - \frac{1}{8}\|\Delta_h \tilde{\boldsymbol{d}}^{n+1}\|_2^2 - 2\|\mathcal{N}_1^{n+1}\|_2^2 \\
&\geq \tfrac{7}{8}\|\Delta_h \tilde{\boldsymbol{d}}^{n+1}\|_2^2 - 18\varepsilon^{-4}((M_0^{(6)})^2 + (C^*)^2)^2(\|\tilde{\boldsymbol{d}}^{n+1}\|_2^2 + \|\nabla_h \tilde{\boldsymbol{d}}^{n+1}\|_2^2) - 4\varepsilon^{-2}\|\tilde{\boldsymbol{d}}^n\|_2^2. \quad (4.52)
\end{aligned}$$

For the nonlinear term $\langle \nabla_h \cdot (\tilde{\boldsymbol{d}}^n \overline{\boldsymbol{U}}^{n+1}), \Delta_h \tilde{\boldsymbol{d}}^{n+1} \rangle_C$, we begin with the following estimate

$$\begin{aligned}
\|\nabla_h \cdot (\tilde{\boldsymbol{d}}^n (\overline{\boldsymbol{U}}^{n+1})^T)\|_2 &\leq C(\|\overline{\boldsymbol{U}}^{n+1}\|_\infty + \|\nabla_h \overline{\boldsymbol{U}}^{n+1}\|_\infty) \cdot (\|\tilde{\boldsymbol{d}}^n\|_2 + \|\nabla_h \tilde{\boldsymbol{d}}^n\|_2) \\
&\leq CC^*(\|\tilde{\boldsymbol{d}}^n\|_2 + \|\nabla_h \tilde{\boldsymbol{d}}^n\|_2), \quad (4.53)
\end{aligned}$$

in which the regularity estimates (4.11) have been utilized. Consequently, we get

$$\begin{aligned}
\langle \nabla_h \cdot (\tilde{\boldsymbol{d}}^n(\overline{\boldsymbol{U}}^{n+1})^T), \Delta_h \tilde{\boldsymbol{d}}^{n+1} \rangle_C &\leq \|\nabla_h \cdot (\tilde{\boldsymbol{d}}^n(\overline{\boldsymbol{U}}^{n+1})^T)\|_2 \cdot \|\Delta_h \tilde{\boldsymbol{d}}^{n+1}\|_2 \\
&\leq 2\gamma^{-1}\|\nabla_h \cdot (\tilde{\boldsymbol{d}}^n(\overline{\boldsymbol{U}}^{n+1})^T)\|_2^2 + \frac{\gamma}{8}\|\Delta_h \tilde{\boldsymbol{d}}^{n+1}\|_2^2 \\
&\leq C(C^*)^2\gamma^{-1}(\|\tilde{\boldsymbol{d}}^n\|_2^2 + \|\nabla_h \tilde{\boldsymbol{d}}^n\|_2^2) + \frac{\gamma}{8}\|\Delta_h \tilde{\boldsymbol{d}}^{n+1}\|_2^2. \quad (4.54)
\end{aligned}$$

The two other terms, namely, $\beta\langle \nabla_h \overline{\boldsymbol{U}}^{n+1} \tilde{\boldsymbol{d}}^n, \Delta_h \tilde{\boldsymbol{d}}^{n+1} \rangle_C$ and $(1+\beta)\langle (\nabla_h \overline{\boldsymbol{U}}^{n+1})^T \tilde{\boldsymbol{d}}^n, \Delta_h \tilde{\boldsymbol{d}}^{n+1} \rangle_C$, could be handled in a more straightforward way:

$$\begin{aligned}
\beta\langle \nabla_h \overline{\boldsymbol{U}}^{n+1} \tilde{\boldsymbol{d}}^n, \Delta_h \tilde{\boldsymbol{d}}^{n+1} \rangle_C &\leq \beta C^*\|\tilde{\boldsymbol{d}}^n\|_2 \cdot \|\Delta_h \tilde{\boldsymbol{d}}^{n+1}\|_2 \\
&\leq 2(\beta C^*)^2\gamma^{-1}\|\tilde{\boldsymbol{d}}^n\|_2^2 + \frac{\gamma}{8}\|\Delta_h \tilde{\boldsymbol{d}}^{n+1}\|_2^2, \quad (4.55)
\end{aligned}$$

$$\begin{aligned}
(1+\beta)\langle (\nabla_h \overline{\boldsymbol{U}}^{n+1})^T \tilde{\boldsymbol{d}}^n, \Delta_h \tilde{\boldsymbol{d}}^{n+1} \rangle_C &\leq (1+\beta)C^*\|\tilde{\boldsymbol{d}}^n\|_2 \cdot \|\Delta_h \tilde{\boldsymbol{d}}^{n+1}\|_2 \\
&\leq 2((1+\beta)C^*)^2\gamma^{-1}\|\tilde{\boldsymbol{d}}^n\|_2^2 + \frac{\gamma}{8}\|\Delta_h \tilde{\boldsymbol{d}}^{n+1}\|_2^2. \quad (4.56)
\end{aligned}$$

The three other nonlinear terms in (4.50) are kept in the current form, since they are able to be cancelled with the nonlinear error terms in the velocity momentum equation. Therefore, a substitution of (4.51), (4.52), (4.54)-(4.56) into (4.50) yields

$$\begin{aligned}
&\|\nabla_h \tilde{\boldsymbol{d}}^{n+1}\|_2^2 - \|\nabla_h \tilde{\boldsymbol{d}}^n\|_2^2 + \frac{5}{4}\gamma\Delta t\|\Delta_h \tilde{\boldsymbol{d}}^{n+1}\|_2^2 + 2\Delta t\langle \tilde{\boldsymbol{u}}^{n+1}, (\nabla_h \Delta_h \tilde{\boldsymbol{d}}^{n+1})^T \boldsymbol{d}^n \rangle_1 \\
&\quad - 2\Delta t\langle (\beta\nabla_h \tilde{\boldsymbol{u}}^{n+1} + (1+\beta)(\nabla_h \tilde{\boldsymbol{u}}^{n+1})^T)\boldsymbol{d}^n, \Delta_h \tilde{\boldsymbol{d}}^{n+1} \rangle_C \\
&\leq D_{13}^n \Delta t(\|\tilde{\boldsymbol{d}}^n\|_2^2 + \|\tilde{\boldsymbol{d}}^{n+1}\|_2^2) + D_6^n \Delta t(\|\nabla_h \tilde{\boldsymbol{d}}^n\|_2^2 + \|\nabla_h \tilde{\boldsymbol{d}}^{n+1}\|_2^2) + \Delta t\|\nabla_h \tau_d^{n+1}\|_2^2, \quad (4.57)
\end{aligned}$$

with $D_{13}^n = 18\varepsilon^{-4}((M_0^{(6)})^2 + (C^*)^2)^2 + 8\varepsilon^{-2} + C(C^*)^2\gamma^{-1} + 4(2\beta^2 + 2\beta + 1)(C^*)^2\gamma^{-1}$,

$$D_6^n = 18\varepsilon^{-4}((M_0^{(6)})^2 + (C^*)^2)^2 + C(C^*)^2\gamma^{-1} + 1. \quad (4.58)$$

4.4. The convergence result. The following theorem is the main result of this article.

THEOREM 4.1. *Given initial data $\boldsymbol{d}_0, \boldsymbol{u}^0 \in C^6(\overline{\Omega})$, with homogeneous boundary conditions, and p^0 obtained by a discrete solver of (2.27), suppose the unique solution for the Ericksen-Leslie system (1.10)-(1.12) is of regularity class $\mathcal{R}$. Then, provided Δt and h are sufficiently small, for all positive integers n, such that $\Delta t \cdot n \leq T$, we have*

$$\|\tilde{\boldsymbol{d}}^n\|_2 + \|\nabla_h \tilde{\boldsymbol{d}}^n\|_2 + \|\tilde{\boldsymbol{u}}^n\|_2 + \left(\Delta t \sum_{m=1}^n \|\Delta_h \tilde{\boldsymbol{d}}^m\|_2^2\right)^{\frac{1}{2}} \leq C(\Delta t + h^2), \quad (4.59)$$

where $C > 0$ is independent of Δt and h.

Proof. A combination of (4.29), (4.48) and (4.57) reveals that

$$\lambda(\|\tilde{\boldsymbol{d}}^{n+1}\|_2^2 + \|\nabla_h \tilde{\boldsymbol{d}}^{n+1}\|_2^2) - \lambda(\|\tilde{\boldsymbol{d}}^n\|_2^2 + \|\nabla_h \tilde{\boldsymbol{d}}^n\|_2^2) + \|\tilde{\boldsymbol{u}}^{n+1}\|_2^2 - \|\tilde{\boldsymbol{u}}^n\|_2^2 + \|\tilde{\tilde{\boldsymbol{u}}}^{n+1} - \boldsymbol{u}^n\|_2^2$$

$$+ \frac{5}{4}\gamma\lambda\Delta t\|\Delta_h \tilde{\boldsymbol{d}}^{n+1}\|_2^2 + \frac{\nu}{2}\Delta t\|\nabla_h \tilde{\tilde{\boldsymbol{u}}}^{n+1}\|_2^2$$

$$\leq D_1^n \Delta t(\|\tilde{\boldsymbol{d}}^n\|_2^2 + \|\tilde{\boldsymbol{d}}^{n+1}\|_2^2) + D_2^{n+1}\lambda\Delta t\|\tilde{\tilde{\boldsymbol{u}}}^{n+1}\|_4^2 + D_3^{n+1}\lambda\Delta t\|\tilde{\boldsymbol{d}}^{n+1}\|_4^2 + D_4^n\Delta t\|\tilde{\boldsymbol{u}}^n\|_2^2$$

$$+ D_5^{n+1}\Delta t\|\tilde{\tilde{\boldsymbol{u}}}^{n+1}\|_2^2 + D_6^n\lambda\Delta t(\|\nabla_h \tilde{\boldsymbol{d}}^n\|_2^2 + \|\nabla_h \tilde{\boldsymbol{d}}^{n+1}\|_2^2) + D_7^{n+1}\Delta t\|\nabla_h \tilde{\boldsymbol{d}}^{n+1}\|_4^2$$

$$+ D_8^{n+1}\Delta t\|\tilde{\boldsymbol{d}}^{n+1}\|_\infty^2 + D_9^n\Delta t\|\tilde{\boldsymbol{d}}^n\|_4^2 + \Delta t(\lambda\|\tau_d^{n+1}\|_2^2 + \lambda\|\nabla_h\tau_d^{n+1}\|_2^2 + \|\tau_u^{n+1}\|_2^2), \quad (4.60)$$

with $D_1^n = \lambda(D_{11}^n + D_{13}^n) + D_{12}^n$, $\quad D_7^{n+1} = CC_6\varepsilon^{-4}$, $\quad D_8^{n+1} = 2(C_6 + C_7 + C_9)\varepsilon^{-4}$,

$\quad D_9^n = C(C_6 + C_8 + C_{10})\varepsilon^{-4}$, $\hspace{6cm}$ (4.61)

in which we have made use of the fact that $\|f\|_3 \leq C\|f\|_4$, $\|\nabla_h f\|_3 \leq C\|\nabla_h f\|_4$ in the derivation. Furthermore, we notice that, the three highly nonlinear inner product terms, namely,

$$2\lambda\Delta t\langle\tilde{\tilde{\boldsymbol{u}}}^{n+1}, (\nabla_h \Delta_h \tilde{\boldsymbol{d}}^{n+1})^T \boldsymbol{d}^n\rangle_1,$$

$$-2\beta\lambda\Delta t\langle(\nabla_h \tilde{\tilde{\boldsymbol{u}}}^{n+1})\boldsymbol{d}^n, \Delta_h \tilde{\boldsymbol{d}}^{n+1}\rangle_C,$$

$$-2(1+\beta)\lambda\Delta t\langle(\nabla_h \tilde{\tilde{\boldsymbol{u}}}^{n+1})^T \boldsymbol{d}^n, \Delta_h \tilde{\boldsymbol{d}}^{n+1}\rangle_C,$$

exactly cancelled between (4.48) and (4.57). This crucial fact plays an essential role in the convergence analysis.

Meanwhile, we observe that there are five terms involved with $\|\cdot\|_4$ and $\|\cdot\|_\infty$ norms on the right-hand side of (4.61). To deal with these terms, we recall the discrete Sobolev inequalities in Lemma 3.1

$$\|\boldsymbol{d}^k\|_4 \leq C\|\boldsymbol{d}^k\|_6 \leq CC_1(\|\boldsymbol{d}^k\|_2^2 + \|\nabla_h \boldsymbol{d}^k\|_2^2)^{\frac{1}{2}}, \quad \text{for } k = n, n+1, \qquad (4.62)$$

$$D_2^{n+1}\lambda\|\tilde{\tilde{\boldsymbol{u}}}^{n+1}\|_4^2 \leq 2C_2^2 D_2^{n+1}\lambda(\|\tilde{\tilde{\boldsymbol{u}}}^{n+1}\|_2^2 + \|\tilde{\tilde{\boldsymbol{u}}}^{n+1}\|_2^{\frac{1}{2}} \cdot \|\nabla_h \tilde{\tilde{\boldsymbol{u}}}^{n+1}\|_2^{\frac{3}{2}})$$

$$\leq Q_{C_2, D_2^{n+1}, \lambda, \nu}\|\tilde{\tilde{\boldsymbol{u}}}^{n+1}\|_2^2 + \frac{\nu}{4}\|\nabla_h \tilde{\tilde{\boldsymbol{u}}}^{n+1}\|_2^2, \qquad (4.63)$$

$$D_7^{n+1}\|\nabla_h \tilde{\boldsymbol{d}}^{n+1}\|_4^2 \leq 2C_2^2 D_7^{n+1}\|\nabla_h \tilde{\boldsymbol{d}}^{n+1}\|_2^{\frac{1}{2}} \cdot \|\Delta_h \tilde{\boldsymbol{d}}^{n+1}\|_2^{\frac{3}{2}}$$

$$\leq Q_{C_2, D_7^{n+1}, \lambda, \gamma}\|\nabla_h \tilde{\boldsymbol{d}}^{n+1}\|_2^2 + \frac{\gamma\lambda}{4}\|\Delta_h \tilde{\boldsymbol{d}}^{n+1}\|_2^2, \qquad (4.64)$$

$$D_8^{n+1}\|\tilde{\boldsymbol{d}}^{n+1}\|_\infty^2 \leq 2C_3^2 D_8^{n+1}(\|\tilde{\boldsymbol{d}}^{n+1}\|_2^2 + \|\nabla_h \tilde{\boldsymbol{d}}^{n+1}\|_2 \cdot \|\Delta_h \tilde{\boldsymbol{d}}^{n+1}\|_2)$$

$$\leq Q_{C_3, D_8^{n+1}, \lambda, \gamma}(\|\tilde{\boldsymbol{d}}^{n+1}\|_2^2 + \|\nabla_h \tilde{\boldsymbol{d}}^{n+1}\|_2^2) + \frac{\gamma\lambda}{4}\|\Delta_h \tilde{\boldsymbol{d}}^{n+1}\|_2^2, \qquad (4.65)$$

in which Young's inequality has been extensively applied. Consequently, a substitution of (4.62)-(4.65) into (4.60) yields

$$\lambda(\|\tilde{\boldsymbol{d}}^{n+1}\|_2^2 + \|\nabla_h \tilde{\boldsymbol{d}}^{n+1}\|_2^2) - \lambda(\|\tilde{\boldsymbol{d}}^n\|_2^2 + \|\nabla_h \tilde{\boldsymbol{d}}^n\|_2^2) + \|\tilde{\boldsymbol{u}}^{n+1}\|_2^2 - \|\tilde{\boldsymbol{u}}^n\|_2^2 + \|\tilde{\tilde{\boldsymbol{u}}}^{n+1} - \boldsymbol{u}^n\|_2^2$$

$$+ \frac{3}{4}\gamma\lambda\Delta t\|\Delta_h \tilde{\boldsymbol{d}}^{n+1}\|_2^2 + \frac{\nu}{4}\Delta t\|\nabla_h \tilde{\tilde{\boldsymbol{u}}}^{n+1}\|_2^2$$

$$\leq \tilde{D}_1^n \Delta t(\|\tilde{\boldsymbol{d}}^n\|_2^2 + \|\tilde{\boldsymbol{d}}^{n+1}\|_2^2) + D_4^n\Delta t\|\tilde{\boldsymbol{u}}^n\|_2^2 + \tilde{D}_5^{n+1}\Delta t\|\tilde{\tilde{\boldsymbol{u}}}^{n+1}\|_2^2$$

$$+\widetilde{D}_6^n\Delta t(\|\nabla_h\tilde{\boldsymbol{d}}^n\|_2^2+\|\nabla_h\tilde{\boldsymbol{d}}^{n+1}\|_2^2)+\Delta t(\lambda\|\tau_d^{n+1}\|_2^2+\lambda\|\nabla_h\tau_d^{n+1}\|_2^2+\|\tau_u^{n+1}\|_2^2),\ (4.66)$$

with $\widetilde{D}_1^n=D_1^n+CC_1^2(D_3^{n+1}+D_9^n)+Q_{C_3,D_8^{n+1},\lambda,\gamma}, \quad \widetilde{D}_5^{n+1}=D_5^{n+1}+Q_{C_2,D_2^{n+1},\lambda,\nu},$

$$\widetilde{D}_6^n=D_6^n\lambda+CC_1^2(D_3^{n+1}+D_9^n)+Q_{C_2,D_7^{n+1},\lambda,\gamma}+Q_{C_3,D_8^{n+1},\lambda,\gamma}. \tag{4.67}$$

To deal with the term $\|\tilde{\tilde{\boldsymbol{u}}}^{n+1}\|_2^2$ on the right-hand side, we make use of the following inequality

$$\|\tilde{\tilde{\boldsymbol{u}}}^{n+1}\|_2^2\le 2(\|\tilde{\boldsymbol{u}}^n\|_2^2+\|\tilde{\tilde{\boldsymbol{u}}}^{n+1}-\tilde{\boldsymbol{u}}^n\|_2^2), \tag{4.68}$$

so that (4.66) could be rewritten as

$$\lambda(\|\tilde{\boldsymbol{d}}^{n+1}\|_2^2+\|\nabla_h\tilde{\boldsymbol{d}}^{n+1}\|_2^2)-\lambda(\|\tilde{\boldsymbol{d}}^n\|_2^2+\|\nabla_h\tilde{\boldsymbol{d}}^n\|_2^2)+\|\tilde{\boldsymbol{u}}^{n+1}\|_2^2-\|\tilde{\boldsymbol{u}}^n\|_2^2+\|\tilde{\tilde{\boldsymbol{u}}}^{n+1}-\tilde{\boldsymbol{u}}^n\|_2^2$$

$$+\frac{3}{4}\gamma\lambda\Delta t\|\Delta_h\tilde{\boldsymbol{d}}^{n+1}\|_2^2+\frac{\nu}{4}\Delta t\|\nabla_h\tilde{\tilde{\boldsymbol{u}}}^{n+1}\|_2^2$$

$$\le\widetilde{D}_1^n\Delta t(\|\tilde{\boldsymbol{d}}^n\|_2^2+\|\tilde{\boldsymbol{d}}^{n+1}\|_2^2)+\widetilde{D}_4^n\Delta t\|\tilde{\boldsymbol{u}}^n\|_2^2+2\widetilde{D}_5^{n+1}\Delta t\|\tilde{\tilde{\boldsymbol{u}}}^{n+1}-\tilde{\boldsymbol{u}}^n\|_2^2$$

$$+\widetilde{D}_6^n\Delta t(\|\nabla_h\tilde{\boldsymbol{d}}^n\|_2^2+\|\nabla_h\tilde{\boldsymbol{d}}^{n+1}\|_2^2)+\Delta t(\lambda\|\tau_d^{n+1}\|_2^2+\lambda\|\nabla_h\tau_d^{n+1}\|_2^2+\|\tau_u^{n+1}\|_2^2),\ (4.69)$$

with $\widetilde{D}_4^n=D_4^n+2\widetilde{D}_5^{n+1}. \tag{4.70}$

As a result, under the constraint that $2\widetilde{D}_5^{n+1}\Delta t\le 1$, we are able to apply the discrete Gronwall inequality and obtain the desired convergence result (4.59). This finishes the proof of Theorem 4.1. □

REMARK 4.1.   In the classical Ericksen-Leslie system, if one denotes the left-hand side of (1.3) for the director as $\hat{\boldsymbol{d}}$, the standard expression of the dissipative stress due to the nematic (with a particular choice of the Leslie coefficients) becomes

$$T_v=\beta\hat{\boldsymbol{d}}\otimes\boldsymbol{d}+(\beta+1)\boldsymbol{d}\otimes\hat{\boldsymbol{d}}.$$

This expression only involves first order derivatives; in particular, weak statements of the equation for $\boldsymbol{u}$ only involve first order derivatives, and many existing finite element numerical schemes have been based on such a classical formulation. On the other hand, a theoretical justification of energy stability for these numerical formulations turns out to be very challenging, due to the highly nonlinear nature of the system. Instead, we make use of a non-standard reformulation (1.10)-(1.12), in which the vector chemical potential $\boldsymbol{\mu}$ has played a key role in both the momentum equation and the dynamical equation for the director field. At a first glance, this reformulation has introduced a term $(\nabla\boldsymbol{\mu})\boldsymbol{d}$, which is involved with the third order spatial derivative of $\boldsymbol{d}$, and this fact seems to make the corresponding system even more complicated. However, a careful analysis reveals that, such an introduction of $\boldsymbol{\mu}$ makes the proposed numerical scheme (2.20)-(2.24) preserve the energy stability at the theoretical level, due to the cancellation of the coupled terms involved with $\boldsymbol{\mu}$, and the semi-implicit treatment of these coupled terms. In addition, the unique solvability and optimal rate convergence analysis have been been provided in this work. As a result, the proposed numerical scheme (1.10)-(1.12) preserves all three properties at a theoretical level.

   In terms of the practical numerical implementation, such an introduction of third order spatial derivatives, in the form of $(\nabla\boldsymbol{\mu})\boldsymbol{d}$, will not cause any essential difficulty, either. In the finite difference spatial approximation, such an idea has been widely

applied to the single-phase-variable gradient flow coupled with incompressible fluid motion, such as Cahn-Hilliard-Helle-Shaw model [9, 10]; great successes have been reported in these finite difference simulations, and the appearance of $\nabla_h \mu$ has not caused any computational trouble, since an intermediate variable has been introduced to denote μ. In the finite element spatial approximation, a mixed finite element approach has been successfully applied for the corresponding numerical system, and many promising numerical results have been reported for both the Cahn-Hilliard-Helle-Shaw and Cahn-Hilliard-Navier-Stokes system [17, 19, 25, 41], *et cetera*.

For the proposed numerical scheme (2.20)-(2.24) to the Ericksen-Leslie system, the detailed numerical solver and the accuracy test numerical results will be presented in the next section. A very efficient iteration solver will be outlined, and the presented numerical results will demonstrate great promises. In other words, an introduction of third order spatial derivative does not cause any practical computational trouble, if the iteration solver is carefully designed.

5. The numerical solver and the numerical results

5.1. A nonlinear iteration solver. Following the analyses in Section 2, the fully discrete numerical system (2.20), (2.23) and (2.24) could be rewritten as

$$\mathcal{F}_h(\boldsymbol{d}) := \mathcal{G}_h^{-1}\left(\frac{\boldsymbol{d} - \boldsymbol{d}^n}{\Delta t}\right) + \varepsilon^{-2}(|\boldsymbol{d}|^2 \boldsymbol{d} - \boldsymbol{d}^n) - \Delta_h \boldsymbol{d} = 0, \tag{5.1}$$

where the discrete operators $\mathcal{G}_h$ and $\mathcal{L}_h$ are defined as

$$\mathcal{G}_h(\boldsymbol{\mu}) := \nabla_h \cdot (\boldsymbol{d}^n(\mathcal{L}_h \boldsymbol{\mu})^T) + (\beta \nabla_h(\mathcal{L}_h(\boldsymbol{\mu})) + (1+\beta)(\nabla_h(\mathcal{L}_h(\boldsymbol{\mu})))^T)\boldsymbol{d}^n + \gamma \boldsymbol{\mu},$$

$$\frac{\mathcal{L}_h(\boldsymbol{\mu}) - \boldsymbol{u}^n}{\Delta t} + \frac{1}{2}(\boldsymbol{u}^n \cdot \nabla_h(\mathcal{L}_h \boldsymbol{\mu}) + \nabla_h \cdot (\mathcal{L}_h \boldsymbol{\mu}(\boldsymbol{u}^n)^T)) - \nu \Delta_h(\mathcal{L}_h \boldsymbol{\mu})$$

$$= -\nabla_h p^n - \lambda(\nabla_h \boldsymbol{\mu})^T \boldsymbol{d}^n - \lambda \nabla_h \cdot \left(\beta \boldsymbol{\mu}(\boldsymbol{d}^n)^T + (\beta+1)\boldsymbol{d}^n \boldsymbol{\mu}^T\right). \tag{5.2}$$

Notice that both $\mathcal{L}_h$ and $\mathcal{G}_h$ are non-symmetric linear operators, with positive eigenvalues, following the arguments in Section 2. In fact, the following linear iteration algorithm could be applied to solve $\mathcal{G}_h(\boldsymbol{\mu}) = \boldsymbol{g}$ (so that $\boldsymbol{\mu} = \mathcal{G}_h^{-1} \boldsymbol{g}$):

$$(\gamma + \omega)\boldsymbol{\mu}^{(k+1)} = -\nabla_h \cdot \left(\boldsymbol{d}^n \left(\mathcal{L}_h(\boldsymbol{\mu}^{(k)})\right)^T\right)$$
$$+ \left(\beta \nabla_h \left(\mathcal{L}_h\left(\boldsymbol{\mu}^{(k)}\right)\right) + (1+\beta)\nabla_h \left(\mathcal{L}_h\left(\boldsymbol{\mu}^{(k)}\right)\right)^T\right)\boldsymbol{d}^n + \omega \boldsymbol{\mu}^{(k)} + \boldsymbol{g}, \tag{5.3}$$

where $\omega \geq 0$ is an $O(1)$ relaxation parameter and $\boldsymbol{\mu}^{(k)}$ and $\boldsymbol{\mu}^{(k+1)}$ stand for the kth and $k+1^{\text{st}}$ iteration stages in the approximate solution of $\mathcal{G}_h(\boldsymbol{\mu}) = \boldsymbol{g}$, respectively. Extensive numerical experiments have demonstrated that a four iteration loop is sufficient to obtain an exact numerical solution to $\mathcal{G}_h \boldsymbol{\mu} = \boldsymbol{g}$ (up to the machine precision), with the initial guess for $\boldsymbol{\mu}$ taken as the numerical solution at the previous time step. As a result, the computation of $\mathcal{G}_h^{-1} \boldsymbol{g}$ only requires a few Poisson solvers (which are needed in the update of $\mathcal{L}_h(\boldsymbol{\mu})$), and such a linear iteration turns out to be a very efficient algorithm.

Meanwhile, it is observed that the original numerical system (5.1) is nonlinear, due to the nonlinear chemical potential part $\varepsilon^{-2}|\boldsymbol{d}|^2 \boldsymbol{d}$. On the other hand, we also notice that, the implicit part of the full chemical potential appearing in (5.1), namely $\varepsilon^{-2}|\boldsymbol{d}|^2 \boldsymbol{d} - \Delta_h \boldsymbol{d}$, corresponds to a discrete convex energy. Motivated by this fact, we apply a preconditioned steepest descent (PSD) iteration algorithm to solve for (5.1).

The essential idea of the PSD solver is to use a linearized version of the nonlinear operator as a pre-conditioner. Specifically, the preconditioner, $\mathcal{J}_h$ is defined as

$$\mathcal{J}_h[\psi] := \frac{1}{\Delta t}\mathcal{G}_h^{-1}\psi + \varepsilon^{-2}\psi - \Delta_h\psi, \tag{5.4}$$

and is a linear operator with positive eigenvalues. Specifically, this "metric" is used to find an appropriate search direction for the steepest descent solver. Given the current iterate $\boldsymbol{d}^{(k)}$, we define the following *search direction* problem: find $\boldsymbol{q}^{(k)}$ such that

$$\mathcal{J}_h\boldsymbol{q}^{(k)} = \boldsymbol{r}^{(k)}, \quad \boldsymbol{r}^{(k)} := \mathcal{F}_h(\boldsymbol{d}^{(k)}), \tag{5.5}$$

where $\boldsymbol{r}^{(k)}$ is the nonlinear residual of the kth iterate $\boldsymbol{d}^{(k)}$. In fact, this equation can be efficiently solved using the Fast Fourier Transform (FFT). Subsequently, the next iterate is obtained as

$$\boldsymbol{d}^{(k+1)} := \boldsymbol{d}^{(k)} + \boldsymbol{\alpha}^{(k)}\boldsymbol{q}^{(k)} = (d_1^{(k)} + \alpha_1^{(k)}q_1^{(k)}, d_2^{(k)} + \alpha_2^{(k)}q_2^{(k)})^T, \tag{5.6}$$

where $\boldsymbol{\alpha}^{(k)} = (\alpha_1^{(k)}, \alpha_2^{(k)}) \in \mathbb{R}^2$ is the unique solution to the steepest descent line problem

$$\begin{pmatrix} \left((\mathcal{F}_h(\boldsymbol{d}^{(k)} + \boldsymbol{\alpha}^{(k)}\boldsymbol{q}^{(k)}))_1, q_1^{(k)}\right) = 0, \\ \left((\mathcal{F}_h(\boldsymbol{d}^{(k)} + \boldsymbol{\alpha}^{(k)}\boldsymbol{q}^{(k)}))_2, q_2^{(k)}\right) = 0. \end{pmatrix} \tag{5.7}$$

This is a nonlinear system for $(\alpha_1^{(k)}, \alpha_2^{(k)})$, in which the linear part corresponds to a matrix with positive eigenvalues (analogous to estimate (2.46)), and the nonlinear part has a positive definite Jacobian matrix (due to the convex energy for the nonlinear implicit part). As a result, such a 2×2 nonlinear system could be very efficiently solved by the Newton iteration.

REMARK 5.1.   The PSD iteration algorithm can be viewed as a quasi-Newton method, with an orthogonalization (line search) step, and $\mathcal{J}_h$ may be viewed as an approximation of the Jacobian. In fact, if $\mathcal{G}_h^{-1}$ is a symmetric operator, the numerical system (5.1) would correspond to the discretization of certain gradient flow, and such a numerical system. could be recast as a minimization of a discrete convex energy functional. In this case, a theoretical analysis ensures a geometric convergence of the iteration sequence; see the related work in [23], and the applications of the PSD solver to various gradient flow models [11, 13, 22, 24]. On the other hand, the operator $\mathcal{G}_h^{-1}$, as introduced in (5.2), is not symmetric, while it is monotone, as stated in (2.46). For the numerical system (5.1) reported in this work, the geometric convergence analysis for the PSD iteration sequence is not directly applicable, while extensive numerical experiments have demonstrated such a geometric convergence rate in the practical computations. Therefore, only five to six iteration stages are needed for the proposed PSD iteration solver in the numerical implementation of (5.1), and the overall computation cost turns out to be of the same level as that for a standard Poisson solver. The theoretical justification of geometric convergence rate for the PSD iteration sequence will be left to the future works, with some technical details expected.

5.2. Convergence test for the proposed numerical scheme.   In this subsection we perform a numerical accuracy check for the proposed numerical scheme (2.20)-(2.24). The computational domain is chosen as $\Omega = (0,1)^2$, and the exact profiles for $\boldsymbol{d}$,

$\boldsymbol{u}$, $\boldsymbol{\mu}$ and p are set to be

$$
\begin{aligned}
\boldsymbol{d}_e(x,y,t) &= \frac{1}{2\pi}\Big(\sin(2\pi x)\cos(2\pi y),\cos(2\pi x)\sin(2\pi y)\Big)^T\cos(t),\\
\boldsymbol{\mu}_e(x,y,t) &= \varepsilon^{-2}(|\boldsymbol{d}_e|^2\boldsymbol{d}_e - \boldsymbol{d}_e) - \Delta\boldsymbol{d}_e,\\
\boldsymbol{u}_e(x,y,t) &= \frac{1}{2\pi}\Big(-\sin(2\pi x)\cos(2\pi y),\cos(2\pi x)\sin(2\pi y)\Big)^T\cos(t),\\
p_e(x,y,t) &= \frac{1}{2\pi}\cos(2\pi x)\cos(2\pi y)\cos(t).
\end{aligned}
\tag{5.8}
$$

The physical parameters are taken as: $\varepsilon = 0.5$, $\nu = 0.5$, $\lambda = 1$, $\beta = -0.5$, and $\gamma = 2$. To make $(\boldsymbol{d}_e,\boldsymbol{\mu}_e,\boldsymbol{u}_e,p_e)$ satisfy the original PDE system (1.10)-(1.12), we have to add an artificial, time-dependent forcing term. The proposed scheme (2.20)-(2.24) can be solved in the rewritten form (5.1), based on the nonlinear PSD iteration algorithm (5.4)-(5.7), combined with linear iteration method (5.3) to obtain $\mathcal{G}_h^{-1}\boldsymbol{g}$.

In the accuracy check for the temporal accuracy, we fix the spatial resolution as $N = 256$ (with $h = \frac{1}{256}$), so that the spatial numerical error is negligible. The final time is set as $T = 1$. Naturally, a sequence of time step sizes are taken as $\Delta t = \frac{T}{N_T}$, with $N_T = 100:100:1000$. The expected temporal numerical accuracy assumption $e = C\Delta t$ indicates that $\ln|e| = \ln(CT) - \ln N_T$, so that we plot $\ln|e|$ vs. $\ln N_T$ to demonstrate the temporal convergence order. The fitted line displayed in Figure 5.1 shows an approximate slope of -0.9861, which in turn verifies a very nice first order temporal convergence order, for the physical variables: d_1, d_2, u and v, in both the discrete L_h^2 and L_h^∞ norms.

In the accuracy test for the spatial accuracy, we set the time size as $\Delta t = h^2$, with $h = \frac{1}{N}$, so that the second order spatial accuracy could be confirmed. Again, the final time is set as $T = 1$. A sequence of spatial resolutions are taken as $N = 48:8:120$. The expected temporal numerical accuracy assumption $e = C(\Delta t + h^2) = C'h^2$ (due to the fact that $\Delta t = h^2$) indicates that $\ln|e| = \ln C - 2\ln N$, so that we plot $\ln|e|$ vs. $\ln N$ to demonstrate the temporal convergence order. The fitted line displayed in Figure 5.2 shows an approximate slope of -2.0092, which in turn verifies a perfect second convergence order in space, for the physical variables: d_1, d_2, u and v.

The initial and final time contour plots for the field $\boldsymbol{d} = (d_1,d_2)^T$ are displayed in Figure 5.3.

Moreover, to illustrate the numerical convergence, we present a comparison between the exact solution and the numerical solution at the final time $T = 1$, for d_1 at the $y = 0.5$ cut, for d_2 at the $x = 0.5$ cut, respectively, in Figure 5.4. A very nice agreement could be observed in the plots.

REMARK 5.2.   The numerical approximation of the Ericksen-Leslie system has been intensely studied over the past two decades. While weak statements involving second order derivatives and various mixed formulations were initially considered, stable formulations with $\boldsymbol{u}$ and $\boldsymbol{d}$ in $H^1(\Omega)$ have been developed, and can be easily coded using the standard finite element spaces available in most existing finite element softwares.

On the other hand, while these existing numerical works for the Ericksen-Leslie system have shown great promise in terms of numerical performance, a theoretical justification of the energy stability and convergence analysis has been very challenging. Among the existing works of theoretical analysis, it is worth mentioning [2], in which a fully discrete finite element scheme to a simplified system is analyzed, without the coupled elastic stress terms, $\beta(\nabla\boldsymbol{u})\boldsymbol{d}$ and $(1+\beta)(\nabla\boldsymbol{u})^T\boldsymbol{d}$. For the regularized system with a penalty approach, the energy stability was proved, an unconditional convergence of finite element solutions towards weak solutions of the continuum PDE model was established in [2], as well as the convergence towards measure-valued solutions of the limiting Ericksen-Leslie model. As a further development, a fully discrete, mixed finite element numerical scheme was proposed for the penalized Ericksen-Leslie system in [26], with semi-implicit treatments for the nonlinear terms. In particular, an optimal rate convergence analysis was reported in [26], with first order convergence rate in
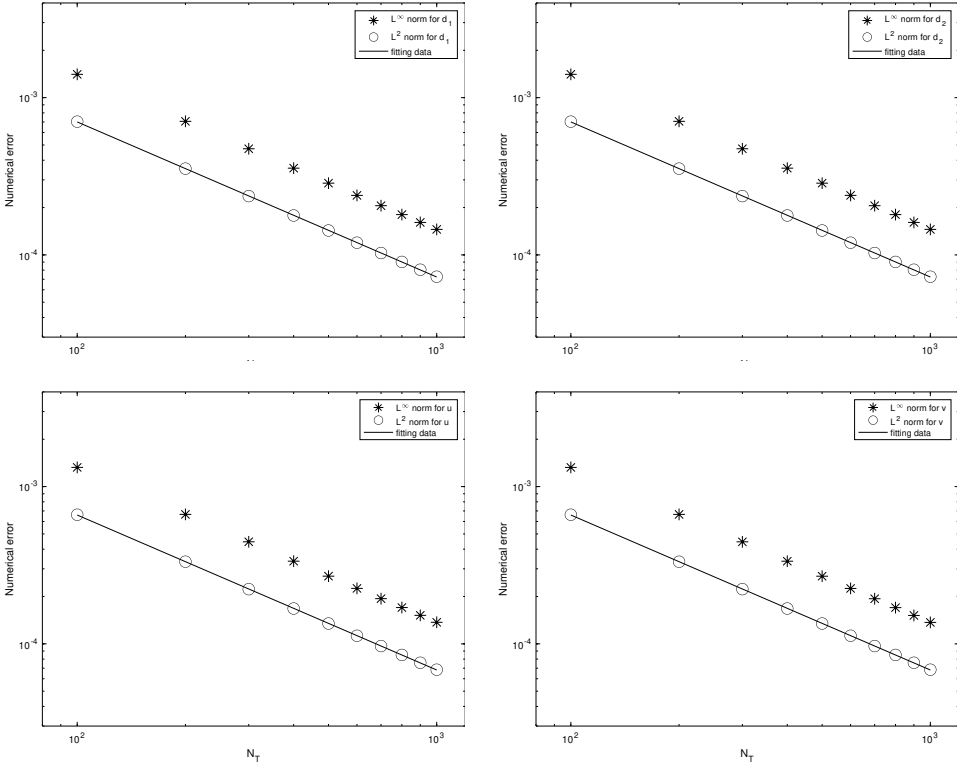
Fig. 5.1: *The discrete L_h^2 and L_h^∞ numerical errors vs. temporal resolution N_T for $N_T = 100$: $100 : 1000$, with a spatial resolution $N = 256$. The numerical results are obtained by the computation using the proposed scheme* (2.20)-(2.24). *The physical parameters are taken as: $\varepsilon = 0.5$, $\nu = 0.5$, $\lambda = 1$, $\beta = -0.5$ and $\gamma = 2$. The numerical errors for the four physical variables: d_1, d_2, u and v, are displayed. The data lie roughly on curves CN_T^{-1}, for appropriate choices of C, confirming the full first-order temporal accuracy of the scheme.*

both time and space. It is observed that the standard L^2 and H^1 bounds for the numerical solution have been derived, while an energy dissipation (in terms of the physical energy) was not reported. In a subsequent work [27], a modified energy stability was proved for the mixed finite element schemes, with an "initial estimate" constraint $h \leq C\varepsilon$ and the "stability" constraint $\Delta t = o(\varepsilon^2 h^2)$. In addition, a few recent works [3, 18, 43, 44, 48] have provided the energy dissipation analysis for the finite element schemes for similarly related phase field model of nematic liquid crystal droplets, and proved that global discrete energy minimizers Γ-converge to global minimizers of the continuous energy, which turn out to be subtle theoretical results. Meanwhile, a theoretical analysis for the Ericksen-Leslie system with the two coupled elastic stress terms seems more complicated, and an optimal rate convergence analysis and error estimate become even more challenging for the full system.

In our work, we make use of a reformulated system (1.10)-(1.12), which includes the highly nonlinear and complicated coupled elastic stress terms. In turn, a fully discrete numerical scheme (2.20)-(2.24) is proposed. This numerical system is linearly coupled, which seems complicated at first glance. However, a careful analysis reveals its rewritten form (5.1), and the nonlinear PSD iteration algorithm (5.4)-(5.7), combined with linear iteration method (5.3) (to obtain $\mathcal{G}_h^{-1}\boldsymbol{g}$) could be applied to implement the fully discrete scheme (2.20)-(2.24). Extensive numerical experiments have indicated a computational cost at the same level as the standard Poisson solvers, which makes the numerical solver very efficient. In addition, perfect first order
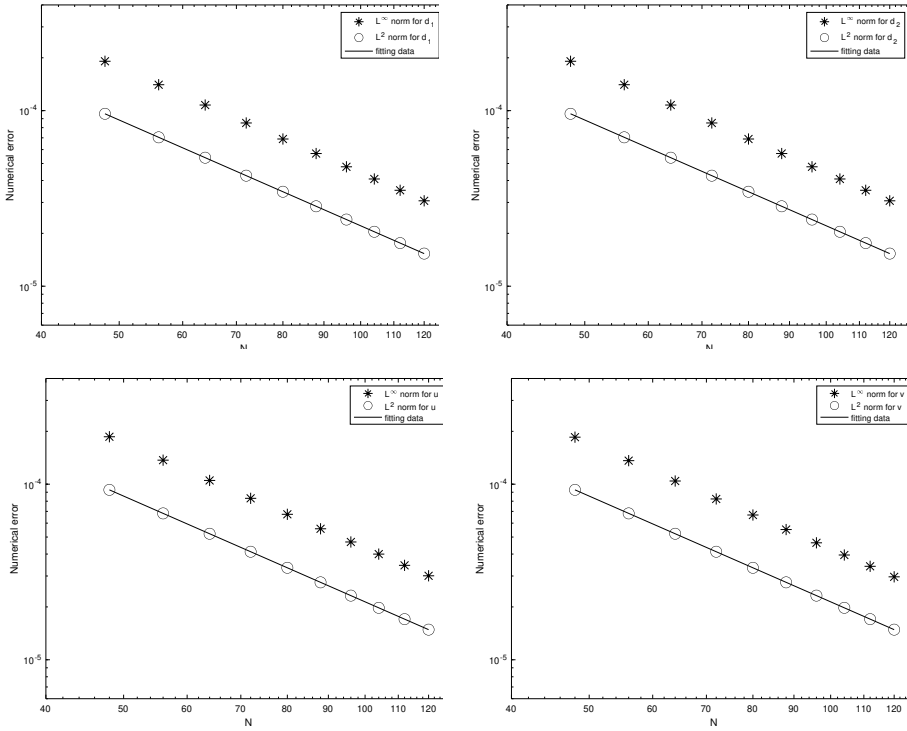
Fig. 5.2: *The discrete L_h^2 and L_h^∞ numerical errors vs. spatial resolution N for $N = 48 : 8 : 120$, and the time step size is set as $\Delta t = h^2$. The numerical results are obtained by the computation using the proposed scheme* (2.20)-(2.24). *The physical parameters are taken as: $\varepsilon = 0.5$, $\nu = 0.5$, $\lambda = 1$, $\beta = -0.5$ and $\gamma = 2$. The numerical errors for the four physical variables: d_1, d_2, u and v, are displayed. The data lie roughly on curves CN^{-2}, for appropriate choices of C, confirming the full second-order spatial accuracy of the scheme.*

d_1 and d_2 at initial time $T = 0$ d_1 and d_2 at final time $T = 1$
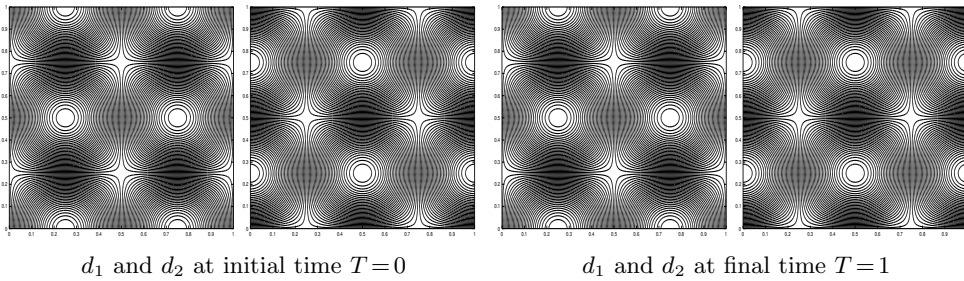
Fig. 5.3: *Contour plots of the computed orientation vector $\boldsymbol{d} = (d_1, d_2)^T$ at the initial time $T = 0$ and final time $T = 1$.*

temporal accuracy and second order spatial accuracy have been reported in the numerical test, and an optimal rate error estimate (in both time and space) has been established. All these facts have demonstrated that, the proposed finite difference scheme (2.20)-(2.24) preserves three perfect theoretical properties: unique solvability, unconditional energy stability, optimal rate convergence estimate, and the formulated numerical solver is very efficient to implement the numerical scheme, with the computational cost at the same level as that of the Poisson
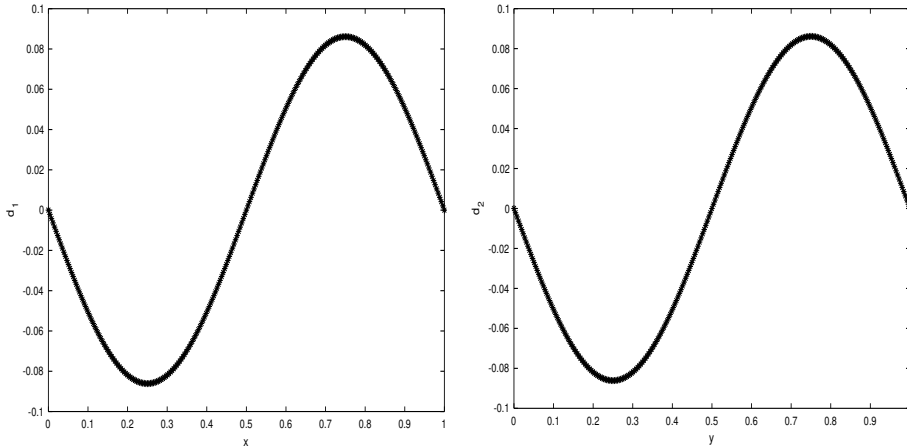
Fig. 5.4: *Left: A comparison between the exact solution and the numerical solution at the final time $T = 1$, for d_1 at the $y = 0.5$ cut. Right: A comparison between the exact solution and the numerical solution at the final time $T = 1$, for d_2 at the $x = 0.5$ cut. The solid lines represent the plot of the exact solution, while the star lines stand for the plot of the numerical solution.*

solvers.

6. Concluding remarks

A semi-implicit numerical scheme is proposed and analyzed for the Ericksen-Leslie system to model nematic liquid crystals. For the penalty function to approximate the constraint $|\boldsymbol{d}| = 1$, a convex-concave decomposition for the corresponding energy functional is applied. Other than this splitting approach, appropriate semi-implicit treatments are adopted to the convection terms, for both the velocity vector and orientation vector, as well as the coupled elastic stress terms. A careful analysis implies that all the semi-implicit terms could be represented as a linear operator of a vector potential, and its combination with the convex splitting discretization for the penalty function leads to a unique solvability analysis for the proposed numerical scheme. A finite difference spatial approximation over staggered mesh points, in which the velocity components and the chemical potential variables are located as different numerical grid points, is applied. The summation by parts formulas and discrete Sobolev inequalities have greatly facilitated the corresponding analysis. A detailed estimate reveals an unconditional energy stability of the numerical system, composed of the kinematic energy and internal elastic energies. Moreover, we provide an optimal rate convergence analysis and error estimate for the fully discrete scheme. In addition, an efficient numerical solver is outlined, based on a preconditioned steepest descent iteration algorithm, combined with a linear iteration method to obtain a linear system solution. The numerical accuracy test results have demonstrated perfect first order temporal accuracy and second order spatial accuracy, which confirm the optimal rate convergence estimate.

Appendix. Proof of Lemma 3.1. For simplicity of presentation, we assume that f is the cell-centered grid function, with homogeneous Neumann boundary condition. Numerical variables evaluated at other mesh points could be analyzed in a similar fashion. We set the

grid f to have the discrete Fourier Cosine transformation as given by

$$f_{i+1/2,j+1/2,k+1/2} = \sum_{\ell,m,n=0}^{N-1} \hat{f}_{\ell,m,n}^N \cos(\ell\pi x_{i+1/2})\cos(m\pi y_{j+1/2})\cos(n\pi z_{k+1/2}). \tag{A.1}$$

In addition, we denote its extension to a continuous function as

$$f_{\mathbf{F}}(x,y,z) = \sum_{\ell,m,n=-K}^{K} \hat{f}_{\ell,m,n}^N \cos(\ell\pi x)\cos(m\pi y)\cos(n\pi z). \tag{A.2}$$

The following estimates could be derived with the help of Parseval's identity; also see the related analysis in [14, 23, 24, 30]:

$$\|f\|_2^2 = \|f_{\mathbf{F}}\|_{L^2}^2 = \sum_{\ell,m,n=0}^{N-1} |\hat{f}_{\ell,m,n}^N|^2, \tag{A.3}$$

$$\frac{2}{\pi}\|\nabla f_{\mathbf{F}}\| \le \|\nabla_h f\|_2 \le \|\nabla f_{\mathbf{F}}\|, \tag{A.4}$$

$$\frac{4}{\pi^2}\|\Delta f_{\mathbf{F}}\| \le \|\Delta_h f\|_2 \le \|\Delta f_{\mathbf{F}}\|. \tag{A.5}$$

On the other hand, we recall a key estimate given by Lemma A.2 in an existing work [24]:

$$\|f\|_p \le \sqrt{\frac{p}{2}}\|f_{\mathbf{F}}\|_{L^p}, \quad \text{in 2-D, } p=4,6,.... \tag{A.6}$$

In addition, such an analysis could also be extended to the 3-D case

$$\|f\|_p \le \left(\frac{p}{2}\right)^{3/4}\|f_{\mathbf{F}}\|_{L^p}, \quad \text{in 3-D, } p=4,6,.... \tag{A.7}$$

The discrete Sobolev inequality (3.13) is a direct consequence of (A.7) (by taking $p=6$), combined with the following inequality in the continuous space: $\|f_{\mathbf{F}}\|_{L^6} \le C\|f_{\mathbf{F}}\|_{H^1}$, as well as the following estimates (coming from (A.4), (A.5)):

$$\|f_{\mathbf{F}}\|_{L^2} = \|f\|_2, \ \|\nabla f_{\mathbf{F}}\| \le \frac{\pi}{2}\|\nabla_h f\|_2, \quad \text{so that } \|f_{\mathbf{F}}\|_{H^1} \le \frac{\pi}{2}\|f\|_{H_h^1}. \tag{A.8}$$

Similarly, the discrete Sobolev inequality (3.14) is a direct consequence of (A.7) (by taking $p=4$), combined with the following inequality in the continuous space:

$$\|f_{\mathbf{F}}\|_{L^4} \le C(\|f_{\mathbf{F}}\| + \|f_{\mathbf{F}}\|^{\frac{1}{4}} \cdot \|\nabla f_{\mathbf{F}}\|^{\frac{3}{4}}), \quad \|\nabla f_{\mathbf{F}}\|_{L^4} \le C\|\nabla f_{\mathbf{F}}\|^{\frac{1}{4}} \cdot \|\Delta f_{\mathbf{F}}\|^{\frac{3}{4}}, \tag{A.9}$$

as well as the estimates in (A.4), (A.5).

The discrete Sobolev inequality (3.16) is a direct consequence of an obvious fact that $\|f\|_\infty \le \|f_{\mathbf{F}}\|_{L^\infty}$, combined with the following inequality in the continuous space:

$$\|f_{\mathbf{F}}\|_{L^\infty} \le C(\|f_{\mathbf{F}}\| + \|f_{\mathbf{F}}\|^{\frac{1}{2}} \cdot \|\Delta f_{\mathbf{F}}\|^{\frac{1}{2}}), \tag{A.10}$$

as well as the estimates in (A.4), (A.5). This finishes the proof of Lemma 3.1.

REFERENCES

[1] S. Badia, F. Guillén-González, and J.V. Gutiérrez-Santacreu, *An overview on numerical analyses of nematic liquid crystal flows*, Arch. Comput. Meth. Eng., 18(3):285–313, 2011. 1

[2] R. Becker, X. Feng, and A. Prohl, *Finite element approximations of the Ericksen-Leslie model for nematic liquid crystal flow*, SIAM J. Numer. Anal., 46:1704–1731, 2008. 1, 5.2

[3] J.P. Borthagaray, R.H. Nochetto, and S. Walker, *A structure-preserving FEM for the uniaxially constrained Q-tensor model of nematic liquid crystals*, Numer. Math., 145:837–881, 2020. 1, 5.2

[4] F. Browder, *Nonlinear elliptic boundary value problems*, Bull. Amer. Math. Soc., 69:962–874, 1963. 2.3

[5] R.C. Cabrales, F. Guilleén-González, and J.V. Gutiérrez-Santacreu, *A time-splitting finite-element stable approximation for the Erickson-Leslie equations*, SIAM J. Sci. Comput., 37:B261–B282, 2015. 1

[6] Y. Cai and J. Shen, *Error estimates for a fully discretized scheme to a Cahn-Hilliard phase-field model for two-phase incompressible flows*, Math. Comp., 87:2057–2090, 2018. 1

[7] R. Chen, W. Bao, and H. Zhang, *The kinematic effects of the defects in liquid crystal dynamics*, Commun. Comput. Phys., 20:234–249, 2016. 1

[8] R. Chen, X. Yang, and H. Zhang, *Second order, linear, and unconditionally energy stable schemes for a hydrodynamic model of smectic-A liquid crystals*, SIAM J. Sci. Comput., 39(6):A2808–A2833, 2017. 1

[9] W. Chen, W. Feng, Y. Liu, C. Wang, and S.M. Wise, *A second order energy stable scheme for the Cahn-Hilliard-Hele-Shaw equation*, Discrete Contin. Dyn. Syst. Ser. B, 24(1):149–182, 2019. 1, 4.1

[10] W. Chen, Y. Liu, C. Wang, and S.M. Wise, *An optimal-rate convergence analysis of a fully discrete finite difference scheme for Cahn-Hilliard-Hele-Shaw equation*, Math. Comp., 85:2231–2257, 2016. 1, 4.1

[11] W. Chen, C. Wang, S. Wang, X. Wang, and S. Wise, *Energy stable numerical schemes for a ternary Cahn-Hilliard system*, J. Sci. Comput., 84:27, 2020. 5.1

[12] K. Cheng, W. Feng, C. Wang, and S.M. Wise, *An energy stable fourth order finite difference scheme for the Cahn-Hilliard equation*, J. Comput. Appl. Math., 362:574–595, 2019. 1

[13] K. Cheng, C. Wang, and S.M. Wise, *An energy stable Fourier pseudo-spectral numerical scheme for the square phase field crystal equation*, Commun. Comput. Phys., 26:1335–1364, 2019. 5.1

[14] K. Cheng, C. Wang, S.M. Wise, and X. Yue, *A second-order, weakly energy-stable pseudo-spectral scheme for the Cahn-Hilliard equation and its solution by the homogeneous linear iteration method*, J. Sci. Comput., 69:1083–1114, 2016. 1, 6

[15] P.A. Cruz, M.F. Tomé, I.W. Stewart, and S. McKee, *Numerical solution of the Ericksen-Leslie dynamic equations for two-dimensional nematic liquid crystal flows*, J. Comput. Phys., 247:109–136, 2013. 1

[16] P.G. de Gennes and J. Prost, *The Physics of Liquid Crystals*, Oxford Science Publications, Oxford, UK, 1993. 1

[17] A. Diegel, X. Feng, and S.M. Wise, *Convergence analysis of an unconditionally stable method for a Cahn-Hilliard-Stokes system of equations*, SIAM J. Numer. Anal., 53:127–152, 2015. 1, 4.1

[18] A. Diegel and S.W. Walker, *A finite element method for a phase field model of nematic liquid crystal droplets*, Commun. Comput. Phys., 25(1):155–188, 2019. 1, 5.2

[19] A. Diegel, C. Wang, X. Wang, and S.M. Wise, *Convergence analysis and error estimates for a second order accurate finite element method for the Cahn-Hilliard-Navier-Stokes system*, Numer. Math., 137:495–534, 2017. 1, 4.1

[20] W. E and J.-G. Liu, *Projection method III: Spatial discretization on the staggered grid*, Math. Comp., 71:27–47, 2002. 2.1

[21] J. Ericksen, *Conservation laws for liquid crystals*, Trans. Soc. Rheol., 5:22–34, 1961. 1

[22] W. Feng, Z. Guan, J.S. Lowengrub, C. Wang, S.M. Wise, and Y. Chen, *A uniquely solvable, energy stable numerical scheme for the functionalized Cahn-Hilliard equation and its convergence analysis*, J. Sci. Comput., 76(3):1938–1967, 2018. 1, 5.1

[23] W. Feng, A.J. Salgado, C. Wang, and S.M. Wise, *Preconditioned steepest descent methods for some nonlinear elliptic equations involving p-Laplacian terms*, J. Comput. Phys., 334:45–67, 2017. 1, 5.1, 6

[24] W. Feng, C. Wang, S.M. Wise, and Z. Zhang, *A second-order energy stable backward differentiation formula method for the epitaxial thin film equation with slope selection*, Numer. Meth. Partial Differ. Equ., 34(6):1975–2007, 2018. 1, 5.1, 6, 6

[25] X. Feng and S.M. Wise, *Analysis of a fully discrete finite element approximation of a Darcy-Cahn-Hilliard diffuse interface model for the Hele-Shaw flow*, SIAM J. Numer. Anal., 50(3):1320–1343, 2012. 4.1

[26] V. Girault and F. Guillén-González, *Mixed formulation, approximation and decoupling algorithm for a penalized nematic liquid crystal model*, Math. Comp., 80:781–819, 2011. 1, 5.2

[27] F. Guillén-González and J.V. Gutiérres-Santacreu, *A linear finite element scheme for a nematic Ericksen-Leslie liquid crystal model*, Math. Model. Numer. Anal., 47:1433–1464, 2013. 1, 5.2

[28] F. Guillén-González and J. Koko, *A splitting in time scheme and augmented Lagrangian method for a nematic liquid crystal problem*, J. Sci. Comput., 65(3):1129–1144, 2015. 1

[29] F. Guillén-González, M.A. Rodríguez-Bellido, and G. Tierra, *Linear unconditional energy-stable splitting schemes for a phase-field model for nematic-isotropic flows with anchoring effects*, Int. J. Numer. Meth. Engg., 108(6):535–567, 2016. 1

[30] J. Guo, C. Wang, S.M. Wise, and X. Yue, *An H^2 convergence of a second-order convex-splitting, finite difference scheme for the three-dimensional Cahn-Hilliard equation*, Commun. Math. Sci., 14:489–515, 2016. 6

[31] F. Harlow and J. Welch, *Numerical calculation of time-dependent viscous incompressible flow of fluid with free surface*, Phys. Fluids, 8:2182–2189, 1965. 2.1

[32] F.H. Lin and C. Liu, *Nonparabolic dissipative systems, modeling the flow of liquid crystals*, Commun. Pure Appl. Math., 48:501–537, 1995. 1

[33] F.H. Lin and C. Liu, *Global existence of solutions for the Ericksen Leslie-system*, Arch. Ration. Mech. Anal., 154:135–156, 2001. 1

[34] F.H. Lin, C. Liu, and P. Zhang, *On hydrodynamics of viscoelastic fluids*, Commun. Pure Appl. Math., 58:1437–1471, 2005. 1

[35] P. Lin and C. Liu, *Simulation of singularity dynamics in liquid crystal flows: A C^0 finite element approach*, J. Comput. Phys., 215:348–362, 2006. 1

[36] P. Lin, C. Liu, and H. Zhang, *An energy law preserving C^0 finite element scheme for simulating the kinematic effects in liquid crystal dynamics*, J. Comput. Phys., 227:1411–1427, 2007. 1

[37] P. Lin and T. Richter, *An adaptive homotopy multi-grid method for molecule orientations of high dimensional liquid crystals*, J. Comput. Phys., 225:2069–2082, 2007. 1

[38] C. Liu and N.J. Walkington, *Approximation of liquid crystal flows*, SIAM J. Numer. Anal., 37:725–741, 2000. 1

[39] C. Liu and N.J. Walkington, *An Eulerian description of fluids containing visco-hyperelastic particles*, Arch. Ration. Mech. Anal., 159:229–252, 2001. 1

[40] C. Liu and N.J. Walkington, *Mixed methods for the approximation of liquid crystal flows*, Math. Model. Numer. Anal., 36:205–222, 2002. 1

[41] Y. Liu, W. Chen, C. Wang, and S.M. Wise, *Error analysis of a mixed finite element method for a Cahn-Hilliard-Hele-Shaw system*, Numer. Math., 135:679–709, 2017. 1, 4.1

[42] G. Minty, *On a monotonicity method for the solution of non-linear equations in Banach spaces*, Proc. Natl. Acad. Sci., 50:1038–1041, 1963. 2.3

[43] R. Nachetto, S.W. Walker, and J. Wang, *A finite element method for nematic liquid crystals with variable degree of orientation*, SIAM J. Numer. Anal., 55(3):1181–1220, 2017. 1, 5.2

[44] R. Nachetto, S.W. Walker, and J. Wang, *The Ericksen model of liquid crystals with colloidal and electric effects*, J. Comput. Phys., 54(4):568–601, 2018. 1, 5.2

[45] R. Samelson, R. Temam, C. Wang, and S. Wang, *Surface pressure poisson equation formulation of the primitive equations: Numerical schemes*, SIAM J. Numer. Anal., 41:1163–1194, 2003. 2.1

[46] R. Samelson, R. Temam, C. Wang, and S. Wang, *A fourth-order numerical method for the planetary geostrophic equations with inviscid geostrophic balance*, Numer. Math., 107(4):669–705, 2007. 2.1

[47] H. Sun and C. Liu, *On energetic variational approaches in modeling the nematic liquid crystal flows*, Discrete Contin. Dyn. Syst., 23:455–475, 2009. 1

[48] S.W. Walker, *A finite element method for the generalized Ericksen model of nematic liquid crystals*, Math. Model. Numer. Anal., 54(4):1181–1220, 2020. 1, 5.2

[49] N.J. Walkington, *Numerical approximation of nematic liquid crystal flows governed by the Ericksen-Leslie equations*, Math. Model. Numer. Anal., 45(3):523–540, 2011. 1

[50] C. Wang and J.-G. Liu, *Convergence of gauge method for incompressible flow*, Math. Comp., 69:1385–1407, 2000. 2.1

[51] H. Wu, X. Xu, and C. Liu, *Asymptotic behavior for a nematic liquid crystal model with different kinematic transport properties*, Calc. Var. Partial Differ. Equ., 45:319–345, 2012. 1

[52] H. Wu, X. Xu, and C. Liu, *On the general Ericksen-Leslie system: Parodi's relation, well-posedness and stability*, Arch. Ration. Mech. Anal., 208:59–107, 2013. 1

[53] K. Xu, M.G. Forest, and X. Yang, *Shearing the I-N phase transition of liquid crystalline polymers: Long-time memory of defect initial data*, Discrete Contin. Dyn. Syst. Ser. B, 15:457–473, 2011. 1

[54] X. Yang, M.G. Forest, H. Li, C. Liu, J. Shen, Q. Wang, and F. Chen, *Modeling and simulations of drop pinch-off from liquid crystal filaments and the leaky liquid crystal faucet immersed in viscous fluids*, J. Comput. Phys., 236:1–14, 2013. 1

[55] S. Zhang, C. Liu, and H. Zhang, *Numerical simulations of hydrodynamics of nematic liquid crystals: Effects of kinematic transports*, Commun. Comput. Phys., 9:974–993, 2011. 1

[56] J. Zhao, X. Yang, Y. Gong, and Q. Wang, *A novel linear second order unconditionally energy stable scheme for a hydrodynamic Q-tensor model of liquid crystals*, Comput. Meth. Appl. Mech. Engg., 318:803–825, 2017. 1

[57] J. Zhao, X. Yang, J. Li, and Q. Wang, *Energy stable numerical schemes for a hydrodynamic model of nematic liquid crystals*, SIAM J. Sci. Comput., 38:A3264–A3290, 2016. 1

[58] J. Zhao, X. Yang, J. Shen, and Q. Wang, *A decoupled energy stable scheme for a hydrodynamic phase-field model of mixtures of nematic liquid crystals and viscous fluids*, J. Comput. Phys., 305:539–556, 2016. 1